# Accepted Manuscript


The challenges in lifetime prediction of oxodegradable polyolefin and biodegradable polymer films

Melissa A.L. Nikolić, Emilie Gauthier, John M. Colwell, Peter Halley, Steven E. Bottle, Bronwyn Laycock, Rowan Truss

PII: S0141-3910(17)30208-2

DOI: 10.1016/j.polymdegradstab.2017.07.018

Reference: PDST 8297

To appear in: *Polymer Degradation and Stability*

Received Date: 20 March 2017

Revised Date: 24 June 2017

Accepted Date: 17 July 2017

Please cite this article as: Nikolić MAL, Gauthier E, Colwell JM, Halley P, Bottle SE, Laycock B, Truss R, The challenges in lifetime prediction of oxodegradable polyolefin and biodegradable polymer films, *Polymer Degradation and Stability* (2017), doi: 10.1016/j.polymdegradstab.2017.07.018.

# The challenges in lifetime prediction of oxodegradable polyolefin and biodegradable polymer films

Melissa A. L. Nikolić[a]*, Emilie Gauthier[b], John M. Colwell[a], Peter Halley[b], Steven E. Bottle[a], Bronwyn Laycock[b], Rowan Truss[b]

[a]Cooperative Research Centre for Polymers, School of Chemistry, Physics and Mechanical Engineering, Queensland University of Technology (QUT), GPO Box 2434, Brisbane, QLD 4001, Australia.

[b]Cooperative Research Centre for Polymers, School of Chemical Engineering, The University of Queensland, St Lucia, QLD 4072, Australia.

*Corresponding author.

Email address: melissa.russo@qut.edu.au (Melissa A.L. Nikolic)

**Keywords:** oxodegradable, biodegradable, hydrolysis, photo-oxidation, thermo-oxidation, polyolefin, titania, poly(butylene adipate-*co*-terephthalate), agricultural film, soil.

## Abstract

The service lifetime of polymer films is controlled by the chemical reactions leading to chain scission and the mediating environmental factors. For application as agricultural cropping film, controlled accelerated degradation is required. For a photo-sensitive linear low density polyethylene (LLDPE) + 1% nano-titania (as the anatase/rutile mixed phase P25), the environmental factors are not only UV dose and temperature but also soil parameters such as moisture and organic material content. This provides a challenge in predicting the useful lifetime from laboratory accelerated ageing studies. To enhance degradation when the (LLDPE + 1% P25) is buried, UV-C pre-irradiation has been shown to accelerate strength loss but the rate of embrittlement is not sufficient for the application as crop propagation film. Biodegradable poly(butylene adipate-*co*-terephthalate) or PBAT has a higher rate of degradation when buried outdoors in soil than when buried under laboratory conditions: The elongation at break fell from 900% to 70% in one month in the field while similar changes required 6 months in the laboratory. The small changes in $\bar{M}_n$ for embrittlement in the field suggests that the loss of mechanical properties was not linked to bulk property changes but rather to surface morphology (cracks and holes) as seen by SEM. This suggests that even in thin films, enzyme-mediated hydrolysis of PBAT is surface controlled. DNA analysis of the soil around the buried films after 35 days ageing outdoors showed fungi play a more dominant role in PBAT biodegradation compared to bacteria. UV

degradation of PBAT film is controlled by the photochemistry of the terephthalate moiety in the polymer and the development of fluorescence is a useful indicator of the extent of photo-degradation.

♯ This paper was, in part, presented on behalf of the authors at MoDeSt 2016 by Professor Graeme George.

## 1.0 Introduction

The food demands of the increasing population of this planet are such that production of many crops must increase by 60% by the year 2050 [1]. Against this is the change in the utilisation of arable land due to climatic change e.g. there have been dramatic reductions in rainfall in the last decade in major grain-growing areas in Western Australia [2]. The net effect is that there need to be changes in production methods as well as opening up of new areas in which food is grown to anticipate the effects of climatic change.

One approach is to create an outdoor, artificial environment that conserves water and favours accelerated production as well as increased reliability of crop yield. Many specialty crops are grown under greenhouse conditions using stabilized clear (or tinted) polyolefin shelters to ensure growth independent of weather variations (especially frost). One approach being researched is to extend the concept of a greenhouse to large scale cropping by using crop propagation film directly above the ground. The aim is to create an environment with a raised air temperature while retaining moisture to encourage early germination of seed and enhance crop growth. It should be noted that this application differs from conventional mulch film where the purpose of opaque, generally black film is to prevent weed growth and allow moisture retention. Unlike crop propagation film, mulch film is punctured at the time of planting seedlings so the plant is exposed to the environment throughout its lifecycle.

At a particular point in the growth cycle, the crop propagation film must be removed to avoid overheating and also not stunt the growth of the plants by creating a physical barrier. This creates an increased cost in labour as well as contributing to the 1.4 million tonnes per year of global post-harvest waste of agricultural plastic that requires disposal. In some regions the disposal of plastic propagation and mulch film is a critical problem [3]. A logical solution to this problem is to use the minimum amount of polymer by having the film thin and tough while being environmentally degradable. For agricultural film application, the question has arisen as to whether it is possible to time this degradation so that, after laying, the film never needs to be retrieved.

This immediately raises challenges in the choice of the polymer and also the control of the rate of the degradation. For example, in crop propagation film the timing of the degradation of the film that forms this “mini-greenhouse” is vital, as shown schematically in Figure 1.

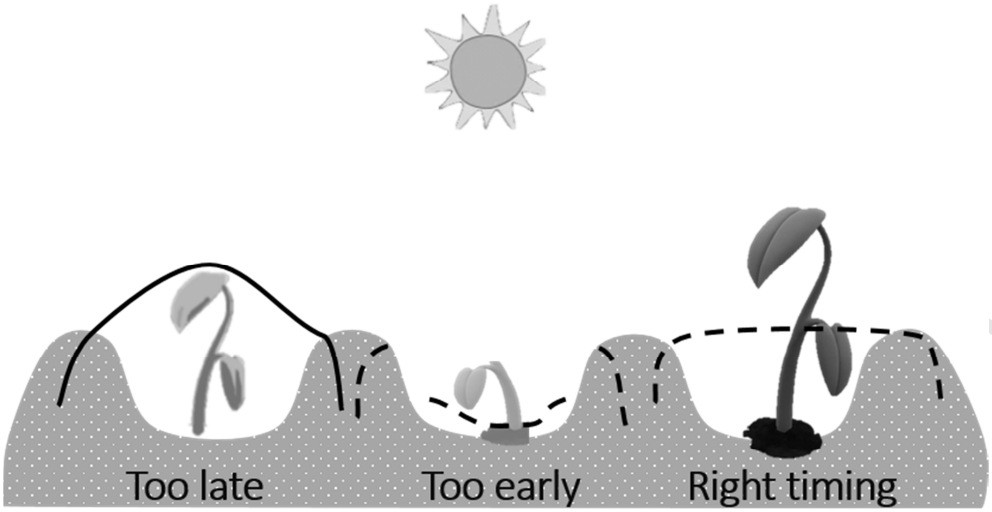


**Figure 1**: **Schematic cross-section of crop propagation film illustrating the importance of the timing of degradation of the film with plant germination and emergence. The diagram to the right is optimum timing, that to the left is too slow to degrade and that in the centre is far too rapid so the benefit is lost.**

The example on the left shows the above-ground degradation of the film is too late and results in loss of the crop due to heat stress as well as being a physical barrier to plant growth; that in the centre shows rapid film degradation before emergence which results in loss of benefit of the film. The example on the right shows maximum benefit by timing degradation after emergence and before rapid growth. It is logical to explore accelerated photo-degradation and/or thermal degradation of polyolefins as the strategy to achieve lifetime control above-ground but this leaves the challenge of the undegraded film below-ground which can foul crop harvesting machinery and require manual removal. One of the key challenges in developing a degradable polymer film for agricultural applications is to have the below-ground section of the film embrittle within the relatively short timeframe required before the field is used for another cropping cycle (typically 6-12 months). Temperatures reached in soil may be in the range of 15 – 30°C, depending on the season and geographical location. Under these conditions, polyethylene film is typically very slow to degrade when buried, with oxidation predominantly occurring via thermo-oxidative processes. These processes are initiated when trace amounts of hydroperoxides (POOH) decompose to produce radicals that lead to degradation of the polymer. This degradation pathway ultimately results in chain scission and loss of mechanical properties to the point of embrittlement. Under standard burial conditions this process is very slow due to the effectiveness of stabilizers in decomposing hydroperoxides to non-radical products or inhibiting the degradation process via reaction with radicals, formed during thermal decomposition of hydroperoxides, to produce benign products. We have found that prodegradants, such as transition metal stearates, that accelerate the oxidation process are typically not

active enough at commercially relevant concentrations to increase the rate of oxidation of agricultural film to a point at which the below-ground sections of film could be ploughed back into the field after a cropping season. Therefore, other methods for accelerating the degradation rate below-ground are required.

Biodegradable films should solve the below-ground degradation issue but the control of above-ground degradation provides a challenge. The time frames of above- and below-ground degradation are totally different leaving a challenge in designing a strong, tough and degradable film which is reliable and cost-effective when used in the wide-ranging global agricultural environments. The most important issue is to tailor the film performance to the needs of the plant since the climate at a site is an average over seasons and local variations in sunlight dose, temperature and rainfall introduce uncertainty in predicting prevailing conditions during a particular growing season.

In this paper we will firstly outline the theoretical framework for lifetime prediction in polyolefin and biodegradable polymer films and then highlight the approaches we have employed to meet the particular requirements for crop propagation film. A particular effort has been made to link laboratory accelerated ageing (controlled UV, temperature, moisture and soil composition) with the performance in the field where each of these factors will vary. The materials studied are:

(i) Oxo-degradable linear low density polyethylene (LLDPE) containing nano-titania for above-ground degradation with a pre-irradiation technology for below-ground degradation.

(ii) Biodegradable poly(butylene adipate-*co*-terephthalate) (PBAT) for combined above- and below-ground degradation.

### 1.1 Lifetime prediction of oxodegradable vs biodegradable polymers

The ultimate fate of a polymer in the environment has often been the concern of regulatory authorities so the focus has been on the rate at which the polymer becomes reduced to carbon dioxide and water rather than the rate at which the polymer loses it mechanical integrity and embrittles. These stages are shown as Stage 2 and Stage 1, respectively, in Figure 2. The time frame for Stage 2 is always much longer for oxodegradable polymers compared to biodegradable polymers and the use of the term “oxo-biodegradable” has been criticised since in the legislative framework for benchmarking biodegradability of polymers against cellulose, even highly oxidised polyolefins will not pass the accepted standard (ISO14855.1:2012. *Determination of the ultimate aerobic biodegradability of plastic materials under controlled composting conditions - Method by analysis of evolved carbon dioxide*). Alternatives to this method have been proposed which are based on biological activity rather than carbon dioxide production (French Standard: AFNOR - AC T51-808. *Assessment of oxobiodegradability of polyolefinic materials in the form of films*). Ultimately the question regarding

the time taken to complete Stage 2 depends on the environment and pre-treatment such as UV exposure that a film receives prior to assessment of biodegradability as well as the rate of the processes and what degree of mineralization is required in the field of use. In agriculture, the toxicity of the system is more important than the time taken to reach total mineralization since small gel particles in the soil may have a beneficial effect on soil condition but a build-up of transition metal salts on prolonged use may need to be monitored [4]. In this paper we will not be assessing the performance of the degradable polymers in Stage 2 of their life cycle.

Only Stage 1 is of concern in this study and we will be considering the factors that control the time taken to embrittle the polymer film. For polyolefins this is most influenced by the rate of peroxidation initiated by UV and thermal prodegradants, while for biodegradable polymers, the rate of hydrolysis is related to the thickness as well as the UV stability. The common features of lifetime prediction are the same for both polymer types since the strength and toughness of a film depends on the molar mass of the polymers, the forces between the chains and the type and extent of crystallinity [5]. When the polymer toughness has decreased to less than 50% of the initial value, embrittlement will soon follow when mechanical stress is applied, although spontaneous embrittlement of a film may require a value as low as 5% of the initial. In principle, determination of the kinetic curve for strength loss over a wide temperature and UV dose range as a function of time would allow the lifetime to be determined by integrating between these limits. For oxodegradable polyolefins the build-up of oxidation products with time of exposure becomes a convenient measure of the approach to failure.

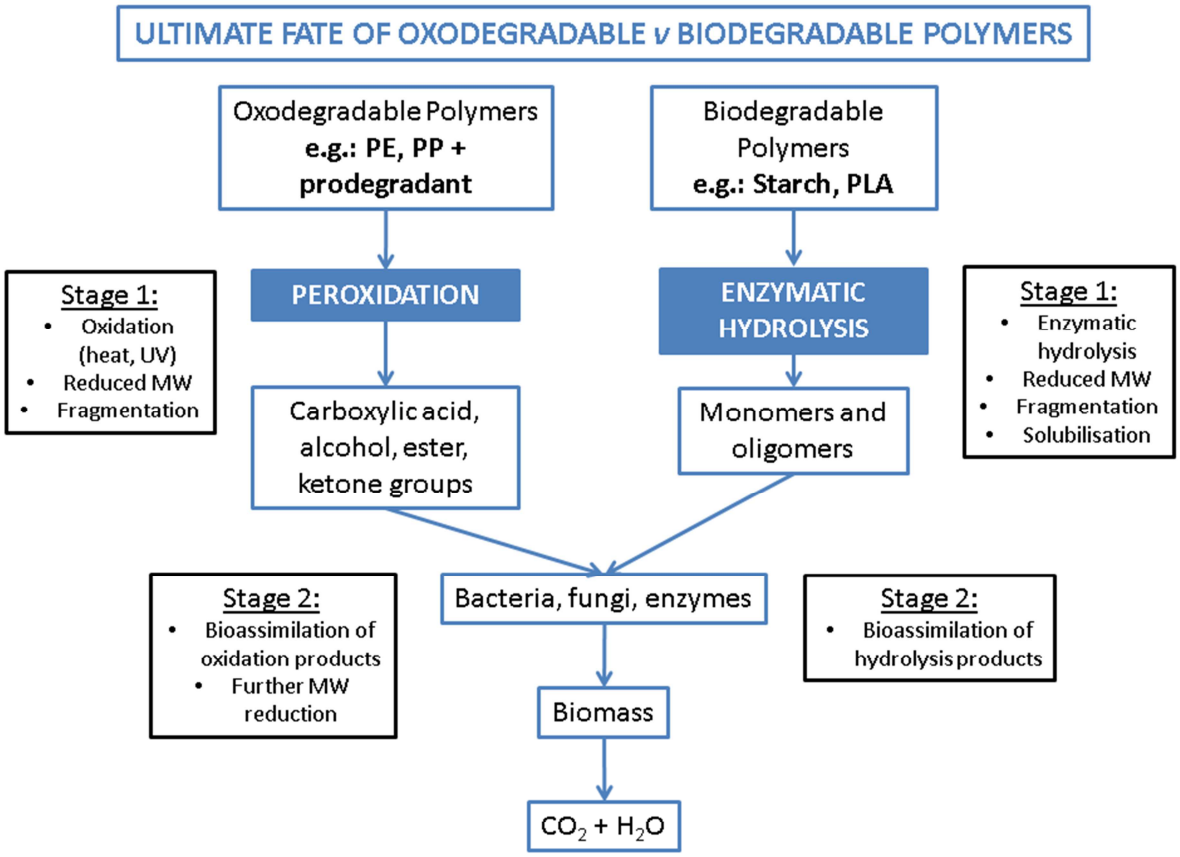


**Figure 2: Schematic of the two stages of degradation contrasting oxo-degradable and biodegradable polymers, adapted from [6]. Control of mechanical integrity of the film is concerned only with the chemical and physical processes in Stage 1.**

Oxodegradable polyolefins use a strategy of enhancement of free-radical peroxidation of the polymer so that the residual stabilizer after processing is soon consumed and enhanced oxidation with chain scission follows. The rate of oxidation is high but in thin polymer films the reaction is not expected to be limited by the availability of oxygen so diffusion limited oxidation should not occur [7]. While homogeneous kinetic models of free radical oxidation of polyolefins have been developed to fit the empirical curves [8], the heterogeneity of degradation means that some areas of the polymer remain undegraded while there are very localized zones of free radical oxidation around points of initiation [9]. As these reactions require oxygen, then only the amorphous fraction of a semi-crystalline polyolefin will oxidize. Within these small oxidizing zones homogeneous kinetics will apply and the full range of free-radical oxidation reactions leading to chain scission or crosslinking will occur. However, this would just lead to localized sub-micron spots of degradation unless the oxidation could spread. A stochastic process therefore follows as these zones then spread and coalesce with others until the degradation reaches a critical size for spontaneous crack formation and ultimately failure

[10]. In the context of agricultural crop propagation film, the initiation will occur by UV exposure above-ground in the presence of a photo-initiator such as titania [11], or iron(III) stearate and degradation below-ground would require enhanced thermal oxidation. This has generally been achieved by having a soluble transition metal salt in a +2 oxidation state (e.g. manganese(II) stearate) that enhances free radical formation by hydroperoxide decomposition, but this process is often prohibitively slow and new strategies described in this paper are required. The particular strategy assessed in this paper is the pre-irradiation of the edges of the film with intense UV-C radiation to create a higher rate of initiation at the temperature of soil burial than would occur for the unirradiated film.

Biodegradable polymers (Figure 2) have functional groups along the backbone (such as esters) which are susceptible to either chemical or enzymatic hydrolysis. In the presence of the appropriate catalyst, random chain scission can take place, so lowering the molar mass. These materials will therefore show much faster degradation when buried but as the process depends on the enzymes present in the soil, the achievement of lifetime control may be difficult without a full understanding of the mechanism. The first factor that emerges is the thickness of the polymer ($L$) compared to the pseudo-first order rate coefficient of hydrolysis ($k'$) and the diffusion coefficient of water in the system ($D$). A critical thickness $L_{crit} = (D/k')^{1/2}$ can be identified below which bulk hydrolysis will occur and above which only surface erosion can take place [12]. In terms of achieving loss of mechanical properties in the time frame of a cropping season this becomes crucial since rapid hydrolysis will result in edge-tearing of the buried film. The mini-greenhouse properties will be lost while slow degradation above-ground will result in polymer that fouls the harvesting machinery. The factors controlling the lifetime of biodegradable polymers are going to be moisture, pH, enzymatic activity, all of which depend on the soil type, in addition to the weather. Mechanistically, random chain scission rather than end-group hydrolysis will lead to more rapid loss of strength and autocatalysis where the acidic products from an enzymatic end-group reaction may then catalyse random scission, providing a level of complexity that may complicate translation from the laboratory to field trials.

In this paper we wish to report the two approaches (oxodegradable LLDPE containing 1wt% titania (P25) and biodegradable PBAT) separately in terms of the challenges that need to be met in obtaining predictable performance based on laboratory and field studies and then look at the way forward in combining the best of both approaches.

## 2.0 Experimental

### 2.1 Oxodegradable linear low density polyethylene (LLDPE)

The base polyethylene used in this study was an LLDPE blend: 93.5% of linear low density PE (Dowlex LLDPE), 5% LDPE and 1.5% polyisobutylene (PIB) (MW 2000 g/mol), where the LDPE

and PIB were used to improve film processing properties and mechanical performance. Aeroxide Degussa P25 titanium (IV) dioxide ($TiO_2$) was supplied by Evonik Australia Pty. Ltd. Prior to processing it was necessary to coat the Degussa P25 $TiO_2$ with Sigmacote® (Sigma-Aldrich) to improve the compatibility with the PE matrix. The mixing ratio was 3.0:2.4 (P25:Sigmacote®) and the particles were stirred in hexane at room temperature prior to solvent removal under vacuum. A laboratory scale single screw extruder (25 L/D Axon BX-25) coupled with a 40 mm diameter die and a film blowing tower was used to prepare 13±3 μm transparent films. Dispersion at a level of 1 wt% P25 addition was measured by TEM [11] and found to consist of dispersed nanoaggregates of dimensions 60 nm to 160 nm compared to the primary P25 particle dimension of ~20 nm.

### 2.1.1 Outdoor Ageing of LLDPE

Films were exposed to natural ageing during the Australian summer (starting on the 26th of February 2014) over different soil types across Australia (Table 1). Two locations separated by 20km were chosen in Queensland: Pinjarra Hills (27.5333°S; 152.9000°E) and Thornlands (27.5500°S, 153.2667°E) and two other sites in Tasmania also 20km apart: Cambridge (42.8367° S, 147.4411° E) and Clifton beach (42.9894° S, 147.5217° E). Soil from each site was characterised by a commercial laboratory, SWEP, in Victoria. The key soil characteristics are summarised in Table 1. Square films of 50x50 cm were laid with buried edges to mimic mini-greenhouse conditions and were monitored every 2 to 3 days. Weather data (solar radiation, temperature, UV index) were collected from weather stations on site, rainfall was collected from the Australian Government Bureau of Meteorology [13] and UV index data were obtained from the Australian Radiation Protection and Nuclear Safety Agency [14].

**Table 1: Characterization of soils used in outdoor and laboratory studies.**

| Texture | Coarse sandy clay loam | Light clay | Sandy loam | Mudstone | Coarse sandy clay loam |
|---|---|---|---|---|---|
| Location | Pinjarra Hills 27.5333°S; 152.9000°E | Thornlands 27.5500°S, 153.2667°E | Cambridge 42.8367° S, 147.4411° E | Clifton 42.9894°S, 147.5217°E | Laboratory |
| Colour | Grey | Grey | Brown | Greyish brown | Brown |
| pH (water) | 7.5 | 5.8 | 5.6 | 5.6 | 6.8 |
| Total organic carbon % | 3.4 | 2.8 | 1.5 | 2.3 | 4.09 |
| % organic matter | 6.8 | 5.6 | 3 | 4.7 | 8.2 |
| Carbon/Nitrogen ratio | 23.5 | 18 | 7.14 | 9.04 | 12 |
| Moisture holding capacity (MHC) | 37.7 ± 0.7' 19.6 ± 3.2[α] | 45.1 ± 0.9' | 34.1 ± 0.7' | 26.5 ± 3.3' | 22.2 ± 0.5[§] |

| | | | | | |
|---|---|---|---|---|---|
| Moisture content (%) | 28.5 ± 1.6[*] | N/A[◊] | N/A[◊] | N/A[◊] | 9.1 ± 0.2[#] |

[*] Soil moisture content was measured, logged and averaged over a 1-week period with two different soil moisture probes.
[#]Sieved soil was dried in an oven at 110°C until a constant mass was obtained and moisture content was calculated accordingly.
[§]MHC was determined according to the method described in ASTM D2980-04.
[α]MHC was determined on a non-sieved soil according to the method described in ASTM D2980-04.
'MHC was measured following the "0 Bar" water holding capacity method.
[◊]Not measured.

### 2.1.2 Activation of edges of oxodegradable LLDPE

Rapid photo-oxidation of oxodegradable LLDPE + 1% P25 was performed with high intensity UV-C radiation in order to assess the feasibility of enhancing the degradation of the buried edges of crop propagation film by activation immediately before laying. Film samples were irradiated in duplicate using a custom-made chamber and parabolic reflector that included 2 x 60W low-pressure mercury vapour lamps (Heraeus). The lamps emitted a line spectrum where approximately 90% of the output is at 254 nm. The setup is described in the patent WO2009021270 A1 [15]. The irradiance at the sample platform was ~100 mW/cm$^2$. Films were irradiated for 10 minutes, which equated to a UV-C dose of 60 J/cm$^2$. To determine if the UV-C activation enhanced thermal degradation when buried, duplicate samples of each film formulation, pre-irradiated and non-irradiated, were mounted onto 35 mm polystyrene slide holders and were aged in a Contherm digital series fan-forced oven, thermostatted at 60°C. It was estimated that this constituted a thermal acceleration factor of ~16 compared to soil burial. Samples were enclosed in a desiccator, where the base was filled with 20 mL of MilliQ water to give an atmosphere of 100% relative humidity (RH). Samples were withdrawn every 48 hours and evaluated for embrittlement and the evolution of carbonyl products using FTIR-ATR (Section 2.3.1).

## 2.2 Biodegradable PBAT

Poly(butylene adipate-*co*-terephthalate) (PBAT) under the trade name Ecoflex F Blend C1200 was supplied by BASF. Prior to film blowing, Ecoflex pellets were dried in a hopper for at least 30 minutes at 70°C. An Axon BX-25 extruder with a L:D ratio of 25:1 and film tower were used to manufacture 400 g of PBAT film with a blowing die temperature of 165°C. The single, 25 mm diameter Gateway screw had several cut flights towards the exit end and was run at 34 rpm. The blow-up ratio was a maximum of 3. Overall film thickness was 29 ± 7 µm, where the thickness of film used in soil burial experiments varied from 25-30 µm and was ~35 µm for Q-Sun weathering experiments (Section 2.2.1).

### 2.2.1 Laboratory ageing of PBAT

For accelerated above-ground ageing, a Q-Sun, model Xe-3-H (Q-Lab) equipped with a chiller was used to simulate day and night cycles (18 hours light followed by 6 hours dark) while controlling the air temperature to 40°C. The irradiance was monitored and automatically adjusted to 0.68 W/m$^2$ at 340 nm. The black panel temperature was 56°C. The UV irradiance was calibrated every 500 h with

an independently calibrated radiometer (CR-20) and the black panel temperature with a calibrated thermometer (CT202). The PBAT films were mounted over 55 mm-diameter x 15 mm-deep glass Petri dishes and held tight using rubber bands, which were replaced every 2-4 ageing cycles. Some dishes were left dry and 5 mL of water was added to some of the Petri dishes to simulate the moisture condensation on the underside of crop propagation film. Water in the Petri dishes was replaced every 2 ageing cycles due to drying out from permeation of water vapour through the films.

For below-ground ageing at a fixed laboratory temperature, six PBAT films of dimensions 15x20 cm were buried in a commercial garden soil (sieved < 2 mm) to a depth of 7-10 cm in a large closed opaque black container at 20.5±0.5$^{o}$C for up to 12 months. The soil characteristics are summarized in Table 1. One film sample was removed every 2 months, washed with water, dried to constant mass in a vacuum oven at 50$^{o}$C, followed by mass measurement with an analytical balance before further characterisation as described in Section 2.3.

#### 2.2.2 Outdoor Burial of PBAT

For outdoor trials, the PBAT film was buried at the Pinjarra Hills test site (Section 2.1.2 and Table 1). Film was collected monthly, except after 1 month of burial where an additional PBAT film and approximately 1 gram of soil were collected and stored immediately on dry ice for DNA analysis of the microbial consortium present in the soil and on the film surface at the time of collection (Section 2.3.6).

### 2.3 Polymer Testing

#### 2.3.1 FTIR Spectra

During accelerated ageing, samples were analysed by using FTIR-ATR and FTIR transmission spectroscopy. FTIR-ATR spectra were collected from both sides of PBAT films: the side facing the lamps and the side facing the Petri dish. FTIR-ATR spectra were collected using a Nicolet 5700 spectrometer. 32 scans were collected at 4 $cm^{-1}$ resolution over the range 4000-650 $cm^{-1}$. Carbonyl Index (CI) values were calculated as a ratio of the height of the carbonyl stretching band at 1712 $cm^{-1}$ to the height of the $CH_2$ scissor band at 1463 $cm^{-1}$ in baseline-corrected spectra using Grams/32 (Galactic Industries Corporation).

FTIR transmission spectra were collected on PBAT films using a Nicolet Nexus 870 FTIR spectrometer. 16 scans were collected at 4 $cm^{-1}$ resolution over the range 4000-400 $cm^{-1}$. Background spectra were collected immediately before each measurement.

#### 2.3.2 Mechanical measurements

Film samples were cut into 25x22 mm strips with the long axis in the transverse direction. Analysis was performed on an Instron 5543 instrument fitted with a 100 N load cell, equipped with pneumatic

grips. The cross head speed of 250 mm/min was chosen based on the ASTM D882 standard test method. Reported values are quoted as the average ± 1 standard deviation of 6-8 replicate samples.

Small samples were also tested for embrittlement by manually applying a small stress perpendicular to the film plane, and the embrittlement point was defined as the ageing time elapsed until the film fractured multi-directionally. At the embrittlement point, the film was too delicate to handle and would break into small flakes.

### 2.3.3 Gel Permeation Chromatography

A Waters GPC system equipped with a Waters 1515 isocratic HPLC pump, Waters 2707 autosampler with a 100 µL injection loop, column heater (30$^{o}$C) and a Waters 2487 dual wavelength absorbance detector (analysis at 254 nm) in series with a Waters 2414 refractive index detector (analysis temperature, 30$^{o}$C) was used for GPC analysis of PBAT samples only. Three consecutive Waters Styragel columns (HR5, HR4, and HR1, all 7.8x300 mm, 5 µm particle size covering the range 100 to 4 000 000 Da), preceded by a Styragel guard column (WAT054405, 4.6x30 mm, 20 µm particle size) were used during analysis. PBAT samples were prepared at 1-2.5 mg/mL in chloroform which was also used as the eluent at 1 mL min$^{-1}$. Molecular weight was determined by calibration against polystyrene narrow-molecular-weight-distribution standards.

### 2.3.4 Scanning Electron Microscopy

Film samples were placed on conducting carbon pads that were adhered to aluminium stubs. The mounted samples were sputter-coated with iridium (thickness 10 nm) using a Quorum Q150T metal coater. The Ir-coated samples were examined with a Hitachi SU3500 SEM (Tungsten filament) at an accelerating voltage of 10 kV and a working distance of 5-6 mm, with a spot size of 40. All images were captured as TIF files at the highest resolution possible. TIF files were post-processed with Paint Shop Pro Version 5 to adjust brightness and contrast where needed.

### 2.3.5 Chemiluminescence

Chemiluminescence measurements were performed using a Lumipol 3 photon-counting instrument (Polymer Institute, Slovak Academy of Sciences) under nitrogen to determine the level of hydroperoxide formed when LLDPE film was UV-C activated. Film samples (~5 mg) were weighed into aluminium pans (9 mm in diameter) and placed in the sample compartment. The nitrogen flow was set to 50 mL min$^{-1}$ and the sample was allowed to equilibrate at 40°C for 30 min before the temperature was ramped up to 250°C at 5°C min$^{-1}$. A 10-second data collection interval was used.

### 2.3.6 DNA analysis

Bacterial 16S rDNA and fungal Internal Transcribed Spacer (ITS) regions within the microbiota on the surface of buried PBAT film and the soil in the vicinity of the buried film (< 2 mm from top of film surface) were assessed and compared for diversity and abundance after 35 days incubation at the

Pinjarra Hills outdoor weathering site. Immediately following collection, samples were placed in sterile tubes or sample bags, stored on dry ice during transit, followed by storage at -80$^{o}$C until further use. Australian Genome Research Facility (AGRF) performed the DNA isolation on both samples of soil and film as described in the Supplementary Information.

#### 2.3.7 UV-Vis spectroscopy

Transmission/reflectance (transflectance) measurements were undertaken using a Varian Cary 5000 UV-Vis-NIR spectrometer. An integrating sphere accessory was used for all measurements, with compressed barium sulfate powder used for baseline measurements and as a reflecting background support for the film samples. During spectral collection, the samples were sandwiched between the quartz window covering the compressed barium sulfate powder and the open sampling window for the integrating sphere accessory. Spectra were collected over the range 200-500 nm at a scan rate of 150 nm/min and a data interval of 1 nm.

## 3.0 Results and Discussion

### 3.1 Outdoor exposure of LLDPE containing P25

Titania (as the anatase:rutile mixed-phase material P25) has been researched as a pro-degradant for crop-propagation film and has been found to become opaque after a short period of UV exposure and before loss of strength. This has been found to offer the unexpected advantage in this application of limiting heat damage to the emerging plants [11]. This opacity has been found to result from the rapid and localized degradation of the polyolefin to carbon dioxide and water around titania nanoparticles. These zones grow and form voids that scatter radiation [11, 16]. This is an advantage in crop propagation film that other prodegradant systems such as transition metal salts (which operate by enhancing decomposition of polymer hydroperoxides and so increasing the rate of oxidation) do not offer. Typically, the addition of 1wt% P25 will reduce the time taken for the LLDPE crop propagation film to embrittle by a factor of ~3 to 4, depending on season. In contrast, the acceleration factor for the same film in a weatherometer may range from ~5 to 8 [11].

This highlights a challenge in predicting the lifetime of polyethylene crop propagation film from weatherometer studies and suggests that there may be other environmental factors to be taken into account other than UV dose. For example, in a recent study of photodegradable LLDPE crop propagation film, it has been found that the properties of the underlying soil had an effect on the time to embrittle [17]. Table 2 shows the time to embrittlement in the present study for the LLDPE film with 1% P25 for four locations when laid above the soil as well as in aluminium holders at two of the locations. The time and dose taken to embrittle LLDPE film without prodegradant when exposed in an aluminium holder was 93 days for a total solar dose of 1535 ± 63 kJm$^{-2}$ at the sub-tropical test site

(Pinjarra Hills). When 1% P25 was included in the film the total solar dose to embrittle reduced to 428 $kJm^{-2}$ indicating an acceleration factor of 3.6.

When the same comparison is made for the other sub-tropical site of Thornlands, the acceleration factor from LLDPE to LLDPE + 1% P25 was 4.3 even though the total solar radiation dose for both films to reach embrittlement was greater at Thornlands. The temperature for the two sites differed by only a few degrees, with Thornlands (Figure 3) being a slightly shaded, slightly cooler, coastal site.

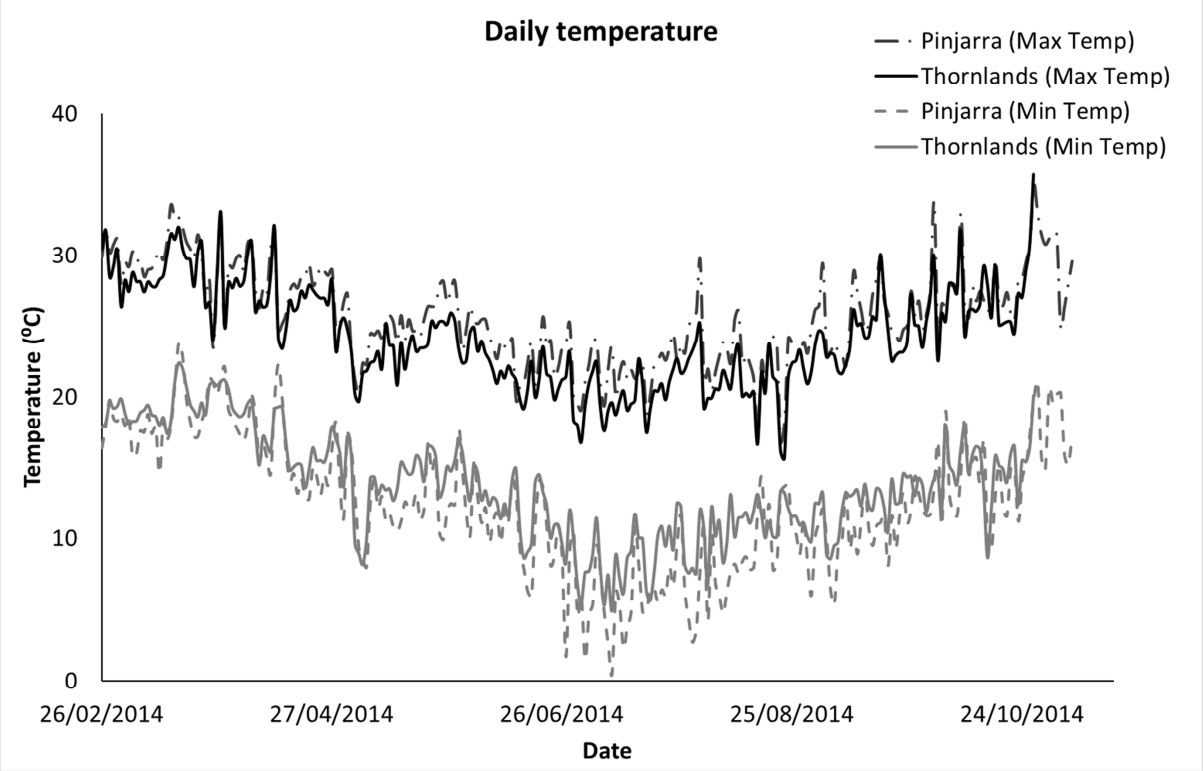


**Figure 3: Daily maximum and minimum temperature at both subtropical sites: Pinjarra and Thornlands, QLD, Australia.**

**Table 2: Time to embrittle (days) and weather parameters for 1% P25 in LLDPE (and LLDPE control films) when exposed outdoors under the different conditions. The ageing data is for 1% P25 in LLDPE films unless otherwise stated.**

| Substrate | Days to embrittle | Total solar radiation dose to embrittle ($MJ/m^2$) | Av. Solar dose rate ($MJ/m^2$/day) | Av. Daily peak UV index | Total rainfall (mm) |
|---|---|---|---|---|---|
| Sandy loam (Cambridge) | 28 | 507±61 | 18.1 | 5.8 | 29 |
| Mudstone (Clifton) | 28 | 697±98 | 24.9 | 5.8 | 26 |
| Coarse sandy clay loam (Pinjarra Hills) | 14 | 313±60 | 22.3 | 9.3 | 16 |
| Aluminium holder (Pinjarra Hills) | 19 | 428±75 | 22.5 | 9.2 | 17 |
| Light clay (Thornlands) | 18 | 383±56 | 21.3 | 9.2 | 26 |
| Aluminium holder (Thornlands) | 20 | 451±20 | 22.5 | 9.1 | 27 |
| LLDPE Control (Al holder, Pinjarra Hills) | 93 | 1535±63 | 16.5 | - | 221 |
| LLDPE Control (Al holder, Thornlands) | 203 | 1950±88 | 9.6 | - | 357 |

The UV exposure of the films in aluminium holders should be the same at the two sites at the same latitude and it is seen that the value of the total solar radiation dose to embrittle LLDPE + 1% P25 for the Pinjarra Hills site (428±75 $MJ/m^2$) and the Thornlands site (451±20 $MJ/m^2$) is identical within a standard deviation. It can be seen from Figure 4 that the dose rates for the two sites are very similar for the first 20 days (indicated by the red square) and for the time taken to embrittle the films with 1% P25. The effect of site on the solar dose rate becomes more pronounced as the trial progresses from late summer through to winter (the flattening of the curve in Figure 4) and is apparent in the embrittlement times of films without prodegradant (the last two entries in Table 2) since the average dose rate at Thornlands is clearly less than Pinjarra Hills (9.6 $MJ/m^2$/day vs 16.5 $MJ/m^2$/day). This can be seen in the time taken to embrittle for the slower-degrading LLDPE control film at Thornlands which increased to 203 days.

This difference may result from the titania-sensitized reaction for free radical generation having a low activation energy compared to hydroperoxide reactions leading to degradation of LLDPE in the absence of catalysts such as transition metals. The lifetime of LLDPE + 1% P25 is thus less sensitive to changes in temperature than LLDPE itself.

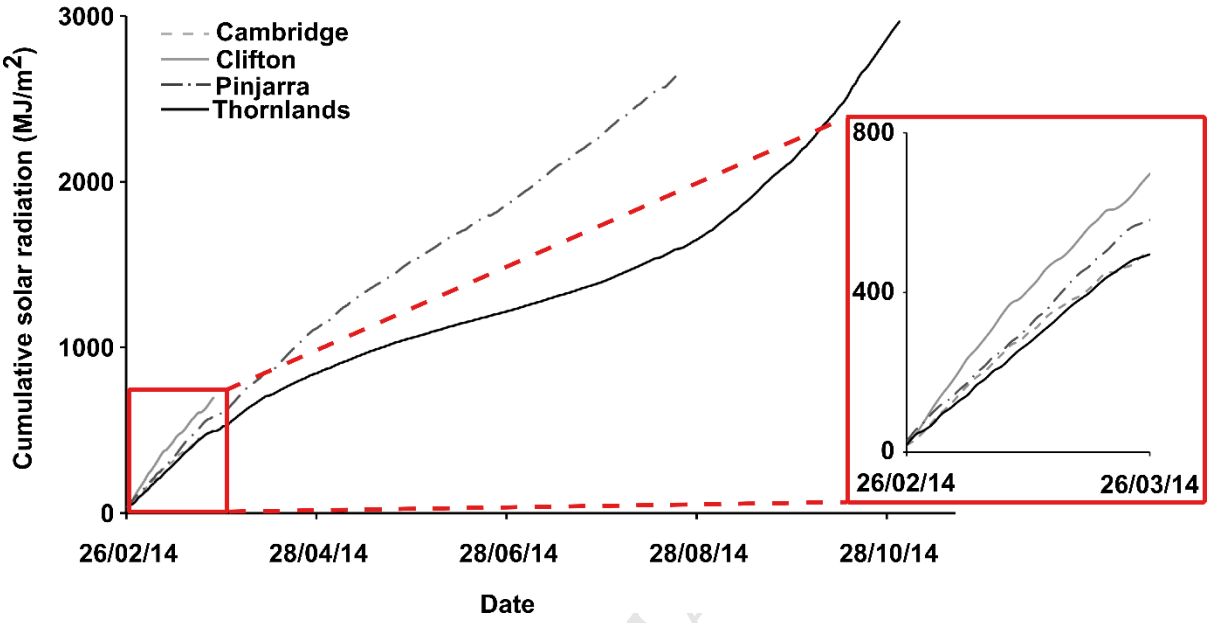


**Figure 4: Cumulative solar radiation for the trial commencing 26 February 2014 and plotted at two-monthly increments as measured at four different exposure sites. The red square is a zoom of the first month of exposure, showing that the dose rates at Thornlands and Pinjarra Hills are very similar up to this time (late summer in the Southern Hemisphere) after which they diverge.**

In principle, as long as allowance is made for the change in dose rate and temperature with time of year, as shown in Figure 4, then it should be possible to predict the time to embrittle the film when used as a crop propagation film at different locations. However, as may be seen from Table 2, when the LLDPE film with 1% P25 was exposed above the sandy loam soil at Pinjarra Hills, the dose to embrittle decreased by a statistically significant amount (27%) compared to the aluminium holder. A decrease of 15% is seen also for the film exposed over the Thornlands soil compared to the aluminium holder, but the effect is more marked when over the coarse sandy loam. The major difference between the conditions of outdoor exposure on an aluminum holder and that when laid onto soil is that the film forms a closed or confined environment. The effect of this is to trap moisture as well as volatiles emitted from the soil. It has been found that the following extra factors need to be taken into account when determining the lifetime of films in the enclosed environment of a crop propagation film:

- There will be an increased temperature and reflected radiation that is soil dependent

- Moisture condensed on the underside of the film can also reflect radiation back into the film
- The organic matter content of the soil and in particular the humic acid component may produce reactive oxygen species (ROS) which may increase the oxidation rate
- Other phenolic substances in soil may have an antioxidant action and reduce the concentration of ROS, so the activity of any soil will be a balance of these competing effects.

The results from the temperate sites in Tasmania (Cambridge and Clifton) show no effect of soil type on the time to embrittle but surprisingly the total solar radiation dose to fail and thus the dose rates are vastly different. The values of dose to embrittle are higher than for the sub-tropical sites, which is likely to be a reflection of the effect of latitude on the UV band edge as indicated by a much lower average daily peak UV index for the sites in Tasmania (Table 2). The UV index is strongly weighted towards wavelengths below ~325 nm, with increasing activity down to 295 nm. This portion of the UV spectrum (UV-B) causes sunburn to human skin, according to the McKinlay-Diffey erythemal action spectrum [18]. Similarly, to the UV index spectrum, P25 is active below 420 nm and has an increasing quantum efficiency for decomposition of organic compounds down to the terrestrial solar cut-off of 295 nm [19]. The UV index has a linear scale, so a relative UV dose can be estimated by taking the ratio of the peak UV indices between sites. Where an average daily peak UV index for the sub-tropical sites (excluding the coarse sandy loam data at Pinjarra Hills and the LLDPE control film data) is compared to that for the sites in Tasmania, a ratio of 0.66:1 is obtained, which is consistent with the ratio for embrittlement times between these sites of 0.68:1. This suggests that the proportion of UV-B within the solar spectrum is the dominant factor in determining degradation rates for P25-containing LLDPE films aged outdoors, and that the temperature differences between the sites had little influence on the time taken for those films to embrittle.

### 3.2 UV-C activation and simulated burial of LLDPE containing P25

Titania photocatalysts such as P25 are regarded as very poor thermal prodegradants [20] so the edges of crop propagation film that are buried would be expected to have a lifetime that is similar to that of LLDPE itself and so constitute an environmental load on the soil due to accumulation of undegraded polyethylene. It has been shown that inclusion of a thermal catalyst for hydroperoxide decomposition such as a transition metal (e.g. manganese(II) stearate) as used in oxodegradable polyolefin formulations in combination with P25 is of little value since there is antagonism due to the redox chemistry of the transition metal and the photo-efficiency of the P25 is drastically reduced [20].

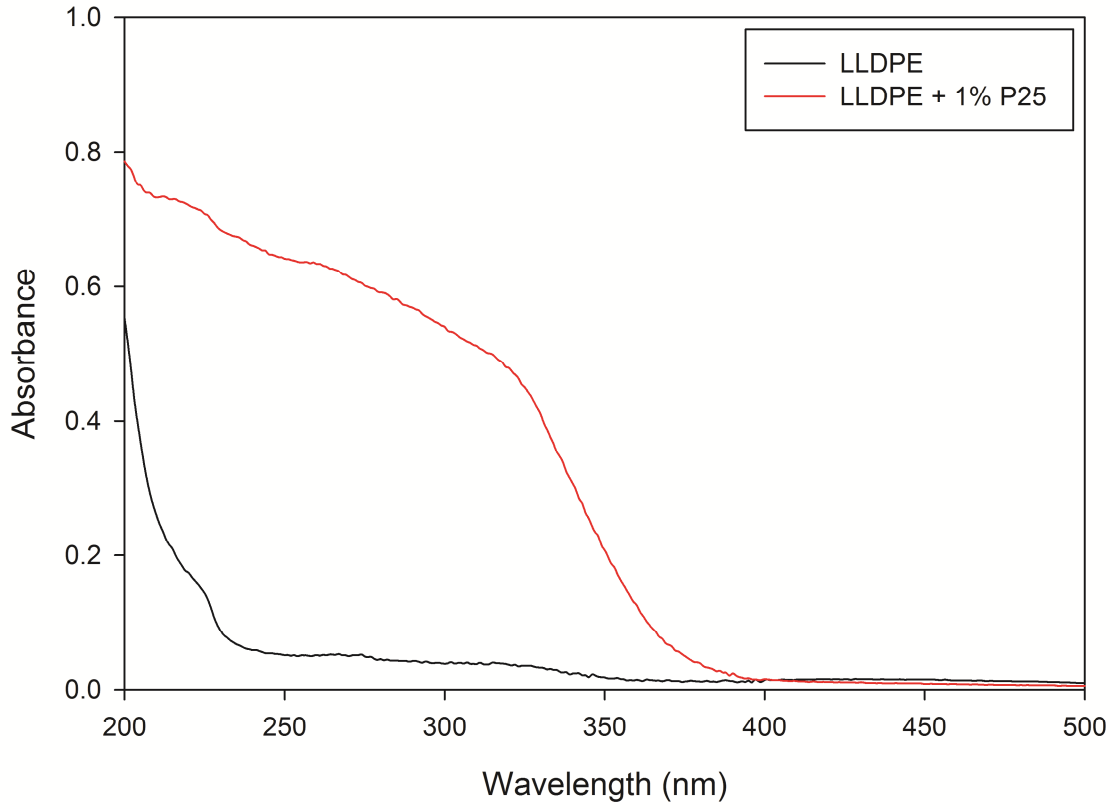


**Figure 5: UV-Vis spectra of LLDPE and LLDPE + 1% P25 films before UV-C irradiation, showing an increasing absorbance of P25 as the wavelength decreases.**

P25 has an activation spectrum extending into the UV-C region, depending on particle size, where it has an increasing quantum efficiency for decomposition of organic compounds as the wavelength decreases from ~420 nm to 300 nm as cited above. P25 also shows increasing absorbance as the wavelength decreases (see initial UV-Vis spectra of the LLDPE and LLDPE + 1% P25 films; Figure 5), so the possibility of pre-activating the LLDPE crop propagation film with low wavelength UV prior to laying was researched. It was found that UV-C pretreatment of polyethylene films both with and without a P25 titania additive led to significant decreases in the time taken to oxidise and embrittle during subsequent ageing in the dark at 60°C and 100% RH (Table 3). These ageing conditions were used as an accelerated model for what would occur during burial of the films in agricultural applications.

**Table 3: Time to embrittlement (Emb.), carbonyl index (CI) at embrittlement and corresponding oxidation induction times for 1% P25 in LLDPE (& LLDPE control films) with and without 60 J/cm$^2$ UV-C irradiation followed by ageing at 60$^o$C and 100% RH in the laboratory.**

| Formulation | No UV-C | | | 60 J/cm$^2$ UV-C | | |
|---|---|---|---|---|---|---|
| | Days to Emb. | CI at Emb. | Oxidation Induction Time at 60$^o$C* (days) | Days to Emb. | CI at Emb. | Oxidation Induction Time at 60$^o$C* (days) |
| LLDPE (control) | 154±6 | 0.37±0.12 | 112.1±7.1 | 35±1 | 0.39±0.17 | 22.6±5.4 |
| LLDPE + 1% P25 | 48±4 | 0.41±0.18 | 35.0±7.6 | 22±2 | 0.23±0.06 | 10.0±1.7 |

*Determined from CI versus time plots by measuring the intercept of the steepest linear slope with an extended baseline.

It is seen from Table 3 that the irradiated LLDPE + 1% P25 has a lifetime of only 14.3% of an LLDPE control film during subsequent thermal ageing, i.e. an acceleration factor of 7 or ≈ 9 when comparing the CI induction times. Surprisingly, it was found that the lifetime and CI induction time of the control film with P25 (i.e. unirradiated) is reduced by a factor of 3.2, so the P25 when dispersed in the way used here (Section 2.1) does initiate thermo-oxidative degradation of LLDPE as well as function as a photo-catalyst. The UV-C pre-irradiation shortens the lifetime of LLDPE during subsequent thermal ageing without the addition of titania and the acceleration factor of 4.4 (in reasonable agreement with the CI induction time acceleration factor of ≈ 5) is higher than for the irradiated sample with 1% P25 when compared to the unirradiated sample.

The IR spectra of the LLDPE films without and with P25 showed only small changes directly after pre-irradiation (before thermal ageing; Figure 6 and Figure 7, respectively). The LLDPE control film showed a small increase in the C-O stretching region of the spectrum (~1260-1000 cm$^{-1}$) suggesting that a small amount of surface oxidation had occurred during UV-C treatment. Conversely, the titania-containing film showed no significant changes in its IR spectrum directly after UV-C irradiation (before thermal ageing).

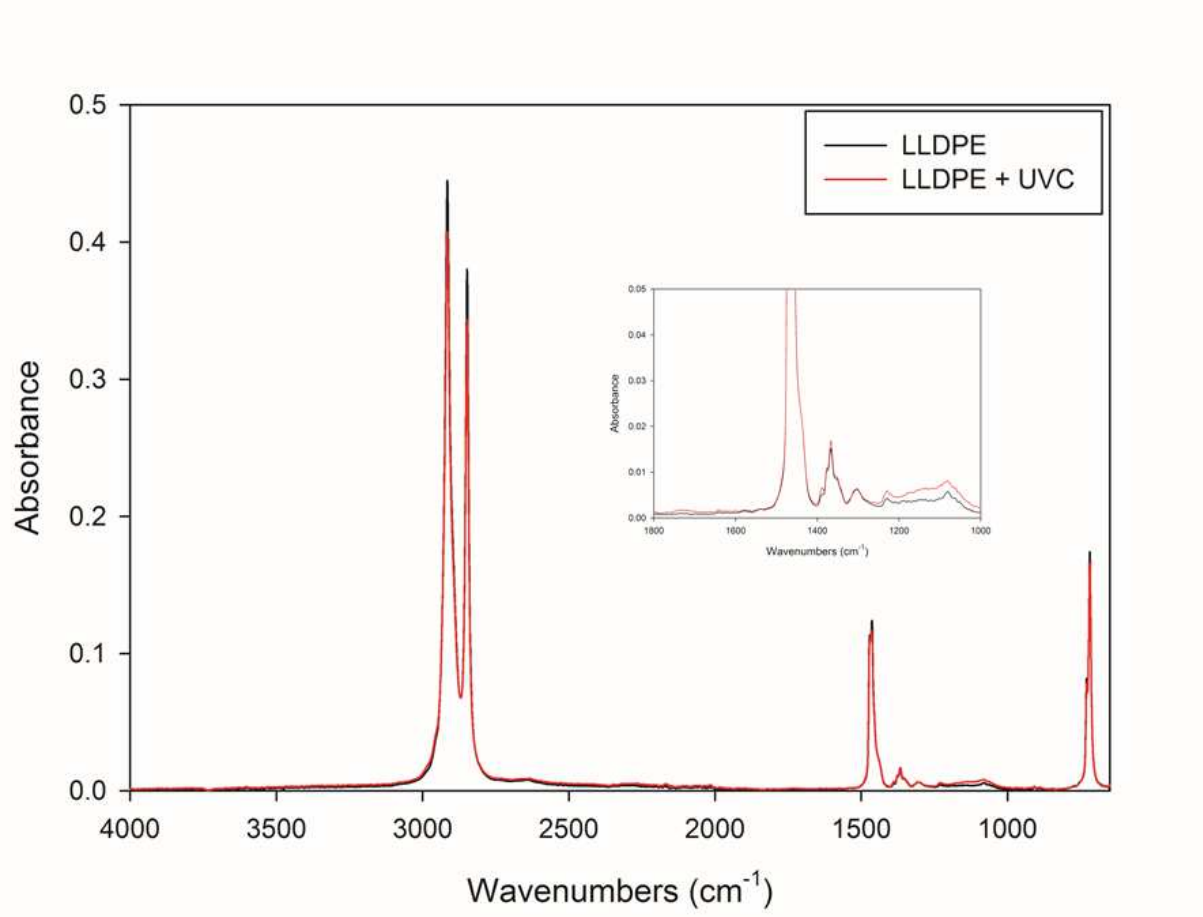


**Figure 6: FTIR-ATR spectra of the LLDPE control film before (black) and directly after (red) UV-C pretreatment showing small changes in the C-O stretching region (~1260-1000 $cm^{-1}$), indicative of minor surface oxidation. See insert for an expanded view of the spectra from 1800-1000 $cm^{-1}$.**

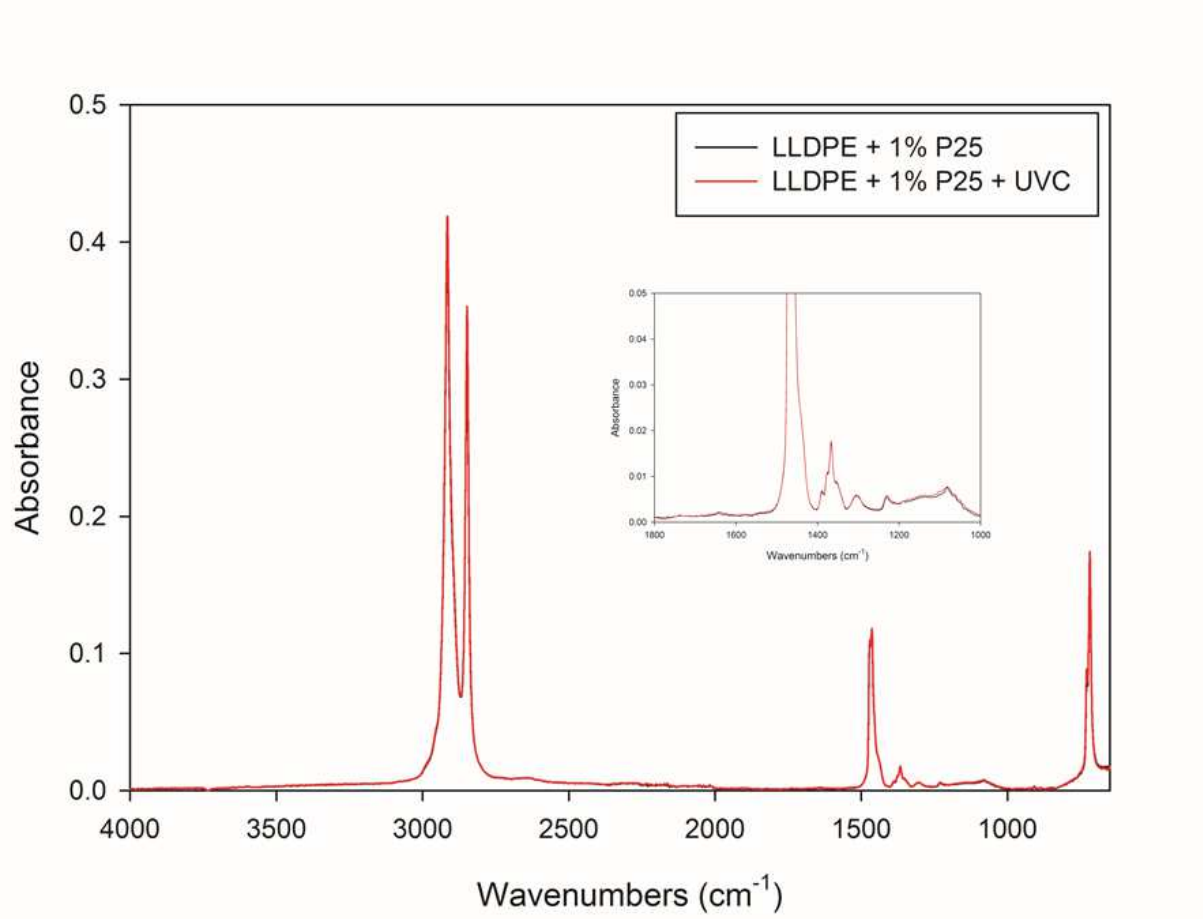


**Figure 7: FTIR-ATR spectra of a titania-containing LLDPE film before (black) and directly after (red) UV-C pretreatment showing no significant changes after irradiation. See the figure insert for an expanded view of the spectra from 1800-1000 cm$^{-1}$.**

The small changes observed directly after UV-C pretreatment, between irradiated and non-irradiated samples using FTIR-ATR do not account for the large changes in the subsequent thermal degradation rate shown in Table 3. Titania is known to cause mineralisation of polyethylene to carbon dioxide and water under photo-irradiation [16], thus leading to a lower than expected carbonyl index as a function of degradation time, which may, in part, help to explain the lack of difference in FTIR-ATR spectra for irradiated and non-irradiated LLDPE + 1% P25 films. To explore this effect further, another technique for assessing the reason for the observed acceleration of subsequent thermal degradation was required. Chemiluminescence is a very sensitive method for detecting oxidation of polyolefins or the presence of degradation initiating species such as hydroperoxides and peroxides when measurements are conducted under an inert atmosphere [21]. Irradiated films (directly after UV-C pretreatment) and non-irradiated films were subjected to chemiluminescence analysis under nitrogen and showed a significant difference in overall emission when films were ramped from 40-220°C (Figure 8). It is also noted that the addition of P25 and the processing by extrusion and film blowing has produced a higher level of hydroperoxides and peroxides than in the control LLDPE film which

has been through the same process. This is consistent with the thermal pro-oxidant effect seen before in Table 3 where the time to embrittle at 60°C was also reduced without pre-irradiation.

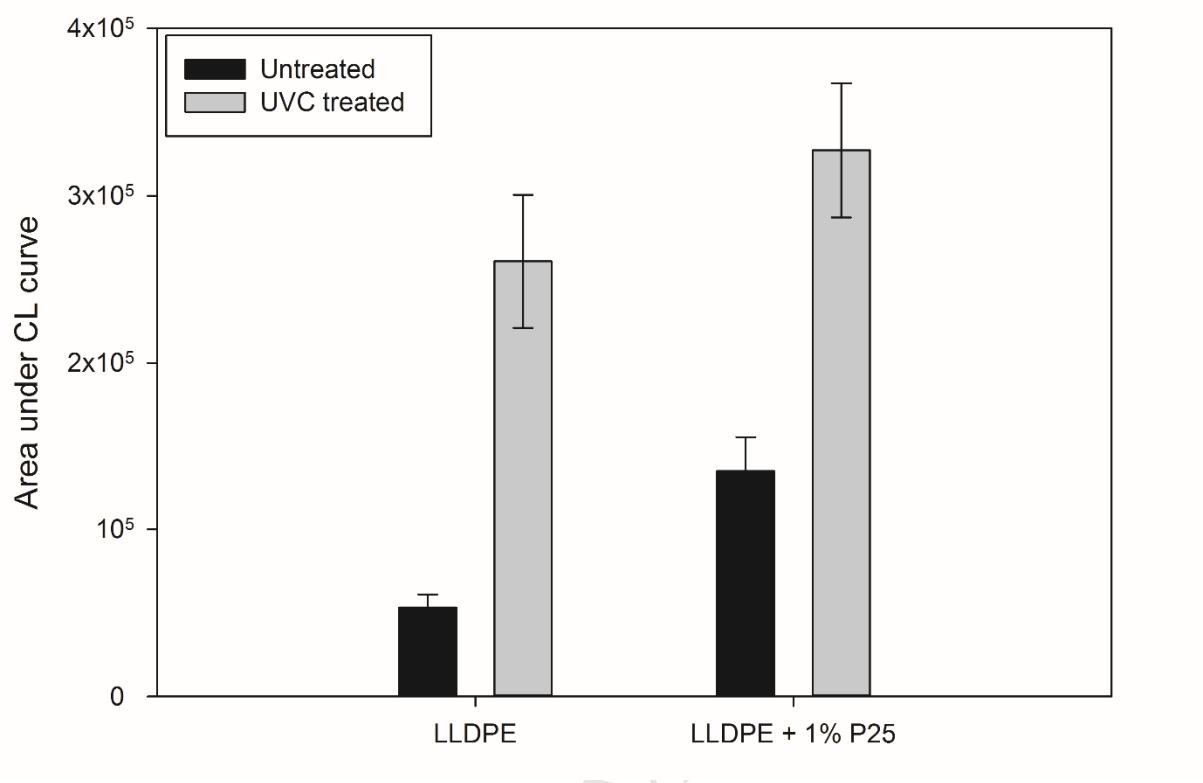


**Figure 8: Area under chemiluminescence (CL) emission curves for LLDPE and 1% P25 in LLDPE films showing a large increase in chemiluminescence directly after UV-C irradiation. Chemiluminescence measurements were performed under a nitrogen atmosphere.**

The relative differences in CL emission between UV-C treated samples and untreated samples are similar to the relative differences in embrittlement times for samples that were UV-C treated and thermally-aged (~4.9 v 4.4 times for the PE control film and ~2.4 v 2.2 times for the titania-containing PE film). Since hydroperoxides and peroxides act as initiating species for thermo-oxidative degradation of polyethylene, these data suggest that the accelerated thermal degradation effect after UV-C pre-irradiation is, at least in part, due to an increased concentration of the (hydro)peroxide species formed during irradiation.

The impact of UV-C pre-irradiation on the degradation of LLDPE and titania-containing LLDPE films was also studied during burial under natural conditions at Pinjarra Hills in Queensland, Australia. Although some changes in elongation-at-break were observed over time (Figure 9), the thermal degradation acceleration effect from UV-C pre-irradiation that was observed for samples aged

in the laboratory was not seen in the field aged samples. For both film types, the changes in elongation-at-break during burial were the same for pre-irradiated and non-irradiated films.

It was therefore concluded that it was unlikely that an oxodegradable formulation that gave the appropriate control of above-ground degradation for crop propagation film would be able to be accelerated sufficiently to achieve the desired level of below-ground degradation for practical applications. There is also the unaddressed issue of the ultimate fate of the material in the soil (Stage 2 in Figure 1). Since agricultural films are buried in fertilised soil where biological degradation may occur, biodegradable materials may provide a solution to this problem, as discussed in the next Section.

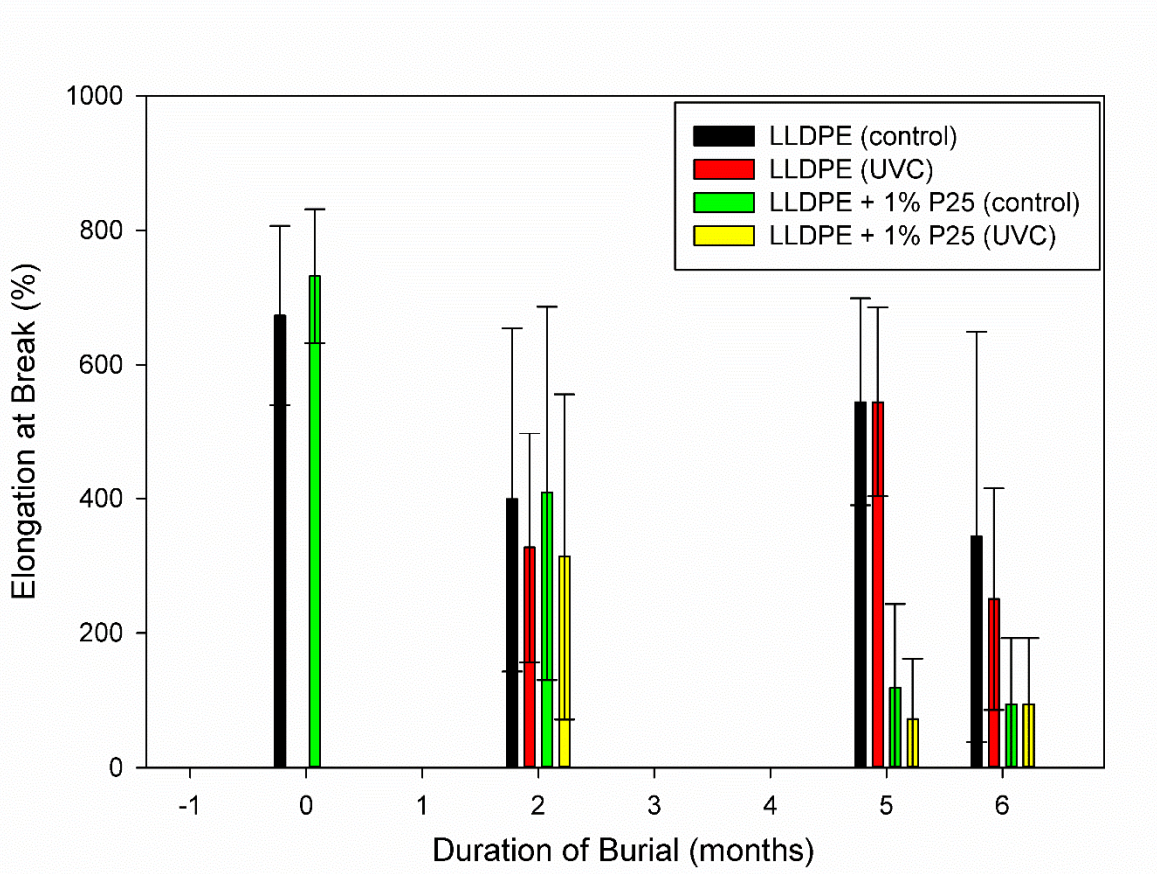


**Figure 9: Evolution of elongation-at-break over burial time for LLDPE and LLDPE + 1% P25 films with and without UV-C irradiation prior to burial in soil at Pinjarra Hills, QLD, Australia.**

### 3.3 Biodegradable PBAT: Assessment of below-ground performance

The applications of many commonly used biodegradable plastics, such as starch and aliphatic polyesters are largely limited by poor mechanical properties, difficulty in processing at scale, sensitivity to moisture and cost [22, 23]. While there has been considerable development in improving

mechanical properties and moisture sensitivity through chemical modification [24], polymer blending [25], barrier coatings [26] and/or the incorporation of nanocomposites [27]; the additional cost of these processes reduce their market competitiveness compared to conventional polyolefin materials. In the 1990s, BASF launched Ecoflex (polybutylene adipate-*co*-terephthalate, PBAT) a synthetic aliphatic-aromatic biodegradable polyester that is certified compostable (ISO14855, DIN EN 13432, ASTM D6400-04, GreenPla), with excellent mechanical properties, is less moisture sensitive compared to traditional biodegradable polymers and can be processed at scale using conventional polyolefin processing equipment that is currently used to produce agricultural film and other film packaging products [28].

Many researchers have investigated the biodegradation of PBAT by evolution of $CO_2$ in compost [29-31] or soil environments [29, 32], demonstrating that PBAT is easily converted to $CO_2$ under compost conditions; however biodegradability is limited in mesophilic soil temperature conditions (20-45$^{o}$C), possibly due to the absence of thermophilic microbes that assimilate PBAT degradation products to $CO_2$ [33]. Other researchers have investigated the impact of environmental factors such as temperature [29, 34], moisture [35], pH [36] and soil microbial activity [29, 37] on the mechanical failure of PBAT by characterising changes in mechanical properties such as elongation-at-break [38] and average molecular weight ($\bar{M}_n$) [33], revealing that soil temperature and moisture greatly impact the overall lifetime of PBAT film.

Although PBAT is referred to as a biodegradable and compostable polymer, Saadi [29] have shown that PBAT biodegradation in a typical soil burial environment at 30$^{o}$C is slow, with only 11% $CO_2$ evolution after 200 days, where to be compliant with aerobic plastic biodegradability standards, such as ASTM 5988-12, more than 70% $CO_2$ evolution is required within 6 months burial in soil, without considering changes in mechanical properties of the polymer that result in mechanical failure (embrittlement). This study investigates the biodegradability of blown PBAT film that has been buried under outdoor weathering conditions at a trial site at Pinjarra Hills in Queensland, Australia and controlled laboratory conditions, with the aim to identify the key parameters and challenges associated with PBAT mechanical failure in soil under mesophilic conditions. It was anticipated that the laboratory conditions would enable the variables to be more carefully controlled.

### 3.3.1 Factors affecting mechanical performance

The factors affecting mechanical performance were summarized in Section 1.1. Applied to a biodegradable polymer such as PBAT these will be temperature, moisture, pH and microbial activity. The temperature of the soil at the outdoor test site (Pinjarra Hills) at a 7 cm depth was highly variable, ranging from approximately 17 to 39$^{o}$C (average 28.3±4$^{o}$C) throughout February 2015 with minimal rainfall; by comparison, the laboratory had a consistent temperature of 21±0.5$^{o}$C and moisture content ranging from 6 to 13%. The change in elongation-at-break and average molecular weight ($\bar{M}_n$) was

measured for PBAT film buried under controlled laboratory or outdoor weathering conditions (Figure 10a & b).

Figure 10a shows that PBAT film buried outdoors for 30 days has lost almost all mechanical integrity with only 70% elongation-at-break remaining in the film without a significant reduction in $\bar{M}_n$. 90 days burial was required for a significant change in $\bar{M}_n$. Under laboratory soil burial conditions (Figure 10b), a similar trend was observed with respect to embrittlement without significant changes in $\bar{M}_n$, although at a significantly slower rate of more than 6 times longer to reach 70% elongation-at-break, suggesting that PBAT hydrolysis throughout the bulk is not the dominant mechanism for mechanical failure.

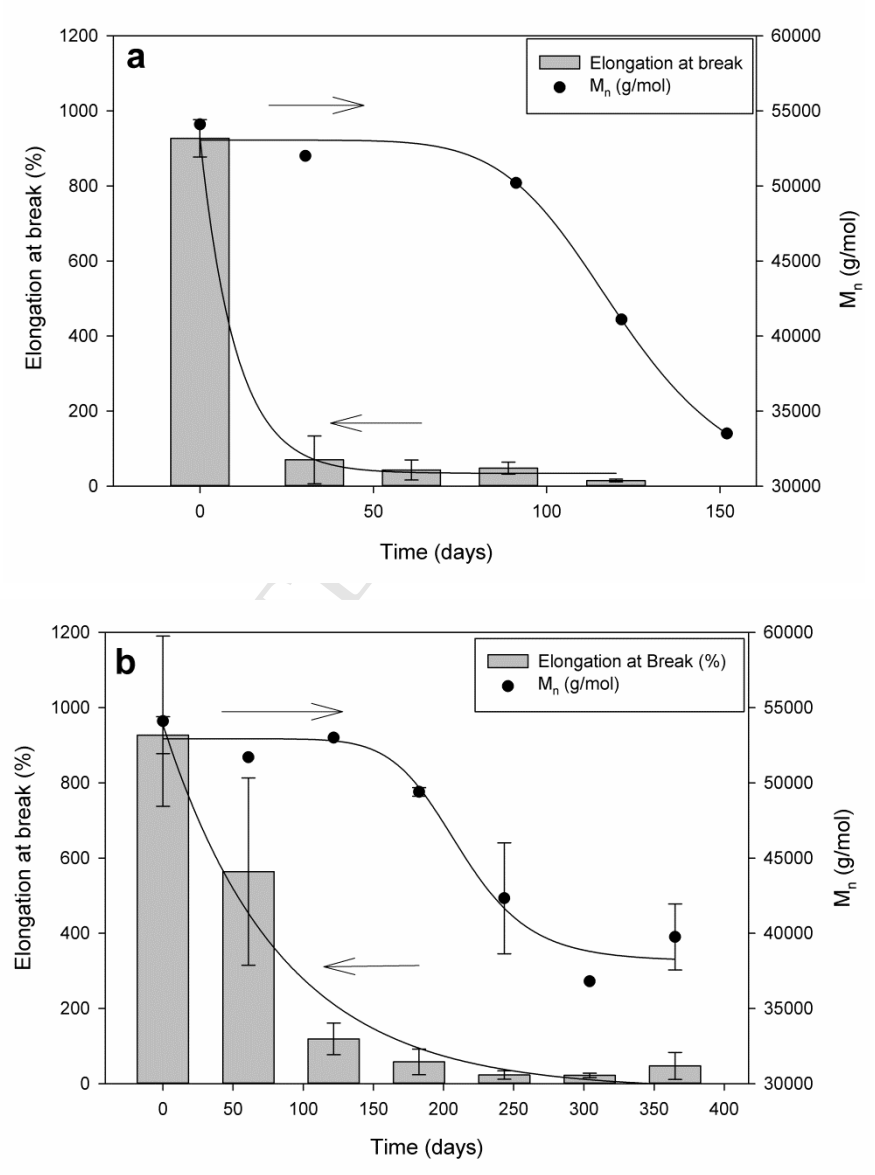


**Figure 10: Observed changes in elongation-at-break and average molecular weight $\overline{M_n}$ for PBAT film buried in soil under (a) outdoor and (b) and laboratory conditions.**

Mass loss measurements of embrittled outdoor buried film (Figure 11) showed only 2% mass loss after 30 days burial outdoors; whereas, under laboratory conditions after double the burial time (60 days), the film was intact with approximately the same amount of mass loss. For laboratory buried film, embrittlement was observed when the sample lost more than triple the amount of mass (6.7% observed at 180 days burial). This suggests that the surface morphology of degraded PBAT film is critical to understanding the mechanism of mechanical failure.

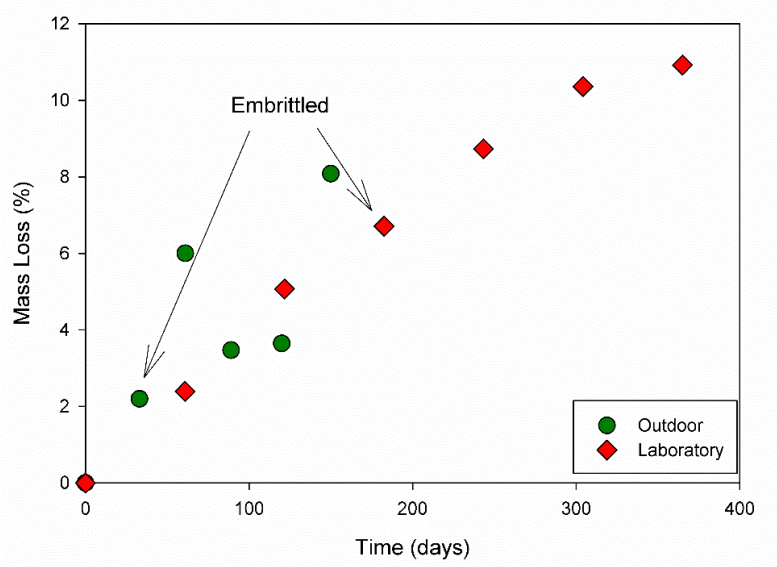


**Figure 11: Mass loss from PBAT film buried in soil under laboratory and outdoor conditions. Once the sample was embrittled, it was difficult to obtain an accurate measure of mass loss due to loss of film in the soil, especially for outdoor aged film.**

### 3.3.2 Influence of surface morphology on mechanical failure

The surface morphology of virgin and buried PBAT films was examined using SEM (Figure 12). After 30 days burial (Figure 12b), the surface morphology of outdoor buried film was dominated by small holes in the machine direction of the film approximately 5x2.5 microns in size, as well as microcracks in the transverse direction up to 50 microns in length.

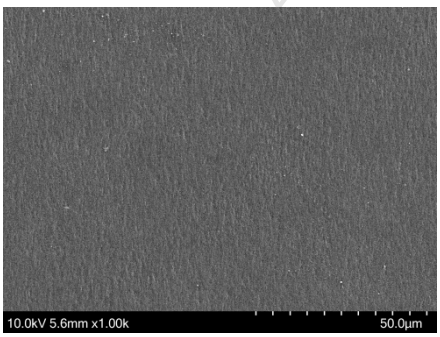


**a: before burial**

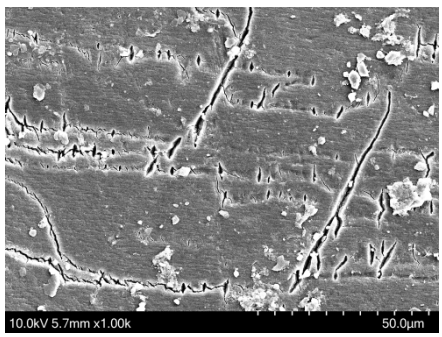


**b: outdoors 30 days**

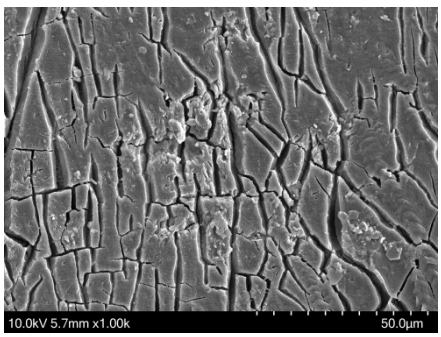


**c: outdoors 60 days**

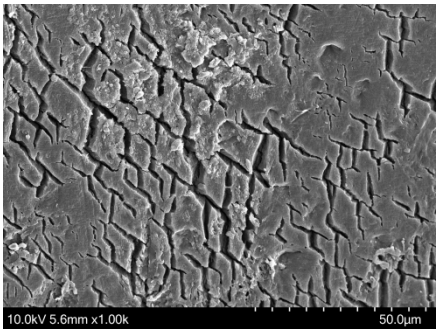


**d: outdoors 90 days**

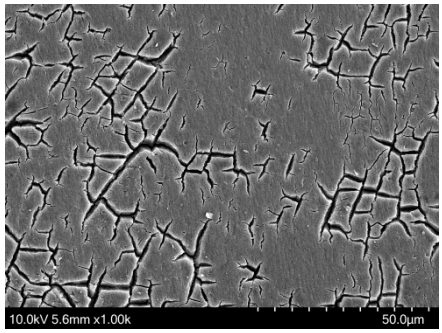


**e: outdoors 120 days**

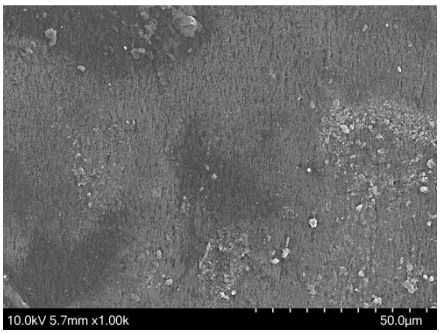


**f: laboratory 60 days**

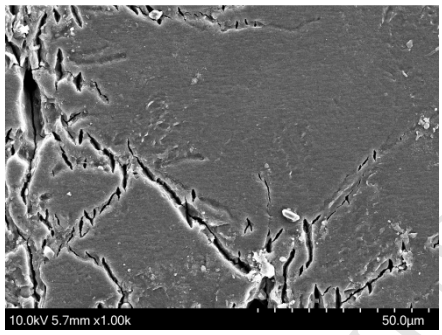


**g: laboratory 120 days**

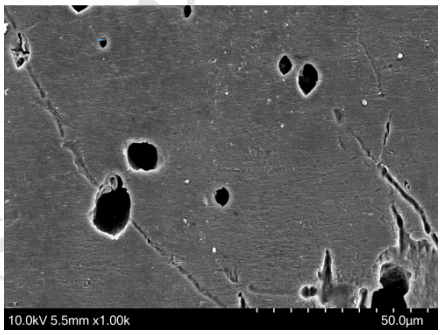


**h: laboratory 180 days**

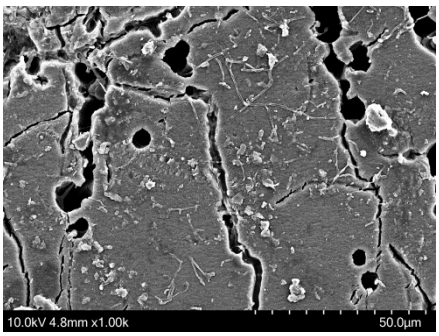


**i: laboratory 240 days**

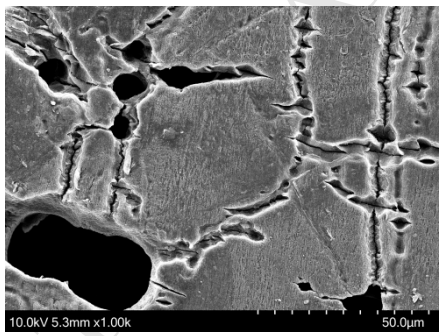


**j: laboratory 300 days**

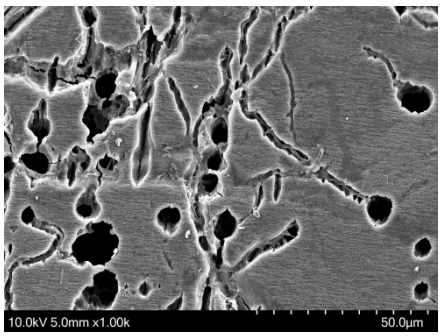


**k: laboratory 365 days**

**Figure 12: SEM micrographs of PBAT film after burial under the conditions indicated. The machine direction of the film is from left to right on each image. Magnification X1000.**

The micrographs suggest that these holes initiate micro-crack formation, as can be seen by micro-cracks that have propagated between these holes up to 60 microns in length. Micro-cracks in the transverse direction are present ranging from 30 to 50 microns with sharp, defined fracture edges. As the time of burial increases to 60, 90 and 120 days outdoors (Figure 12: c-e), the micro-cracks appear to reach deeper into the film and are of a more ordered honeycomb pattern, as micro-cracks coalesce in both the machine and transverse directions. Changes in the surface morphology of laboratory buried film were much slower to evolve compared to outdoors, with few morphological changes after 60 days of burial (Figure 12f), even though the film had lost approximately 2% mass, which was

sufficient mass loss for an outdoor burial film to reach embrittlement. After 120 days of burial (Figure 12g) micro-cracks became evident and showed a similar morphology to what was seen on film buried outdoors after 30 days; however, this surface cracking was not to the extent required to result in mechanical failure. Embrittlement was only observed after 180 days of burial (Figure 12h) at which time many holes were evident on the film surface ranging from 1 – 30 microns, further contributing to a higher mass loss of 6.5% at embrittlement. As the time of film burial increased (Figure 12:i-k) for up to 365 days, holes on the surface can be seen coalescing to form even larger voids, further reducing the elongation-at-break and leading to increased mass loss from the film. The surface morphology of PBAT films aged under thermo-oxidative conditions at 60$^{o}$C and 100% humidity for over 100 days was relatively smooth at embrittlement. This suggest that the morphology of the film surface dominates the mechanism of mechanical failure in soil, which may be linked to the soil microbiota.

### 3.3.3 Influence of soil microbiota on mechanical failure

The results from the SEM analysis suggest that the microbiota of the soil plays a significant role on PBAT lifetime under environmental mesophilic conditions (20 – 45°C). Further examination of the literature has revealed that certain bacterial and fungal strains have been reported to assimilate PBAT under these conditions. Muroi [37] reported SEM micrographs with a micro-cracking pattern on the film surface after 3 months incubation and an approximate mass loss of 1%, very similar to observations reported in this study after 30 days of burial outdoors. Microbial DNA analysis showed that fungi belonging to the phylum Ascomycota were enriched in soil within close proximity to the PBAT film surface, also impacting on the growth of specific fungal species in bulk soil. On the other hand, the bacterial flora community composition present in both bulk soil and in soil in close proximity to PBAT film were not significantly different, suggesting that the presence of PBAT did not strongly influence this community, in turn suggesting that certain fungal species are key to the lifetime of PBAT film in soil under mesophilic conditions.

In order to investigate the efficiency of certain bacterial and fungal strains to biodegrade PBAT in soil under mesophilic conditions, Kasuya [32] investigated the impact of modifying soil microbiota on the biodegradability of PBAT through the isolation of 3 fungal strains belonging to the Ascomycota phylum (NKCM1712, NKCM1713 and NKCM2510) and 2 gram-positive bacterial strains (NKCM2511 and NKCM2512) under aerobic conditions at 30°C. The results showed that the fungal strain NKCM1712 degraded PBAT film most rapidly (3.5 ± 0.3 µg $cm^{-2}h^{-1}$). After 5 days of cultivation, many microcracks had formed heterogeneously over the film surface and by 10 days the film surface was completely covered in microcracks. Phylogenetic analysis based on the Internal Transcribed Spacer (ITS) region revealed that the NKCM1712 strain is closely related to *Isaria fumosorosea* NBRC7562, a pathogen of citrus fruits. Tan [33] have also reported that some mesophiles belonging to the Ascomycota phylum showed hydrolytic activity against PBAT under

mesophilic conditions; however, at higher temperatures (40 – 50°C), thermophilic eubacterial species such as thermophilic actinomycetes were the most crucial microorganisms involved in degrading PBAT. After 21 days of incubation at 30°C the following bacterial, yeast/fungal strains caused more than 1 % mass loss from PBAT film: *Acinetobacter* sp. ATCC 31012, *Aeromonas* sp. ATCC 55641, *Bacillus subtilis* ATCC 6051, *Bacillus subtilis* ATCC 21332, *Delftia acidovorans* soil isolate, *Pseudomonas aeruginosa* PA01, *Pseudomonas fluorescens* ATCC 13525, *Candida bombicola* ATCC 22214, *Paecilomyces lilacinus* ATCC 200182. Gel permeation chromatography results suggested exo-enzyme type degradation, where the microbes hydrolysed the ester bonds at the termini of the polymeric chains preferentially.

Within our study, the differences in bacterial (Figure 13) and fungal (Figure 14) diversity and abundance on the PBAT film surface and soil in close proximity to the film were assessed after 35 days of burial at the outdoor weathering site at Pinjarra Hills. The data in both Figure 13 and Figure 14 has been screened to only include taxa with a relative abundance greater than 0.01 as a way to screen for key species participating in PBAT biodegradation (additional taxon data available in Supplementary Information). The dominant bacteria phyla identified in the soil were Proteobacteria, Actinobacteria, Acidobacteria and a range of unidentified bacteria where only low amounts (<0.01) of specific species within these phyla were on the surface of the PBAT film (with the unidentified bacteria an exception). Muroi [37] reported Proteobacteria, Actinobacteria and Gemmatimonadetes phyla as being present in soil during a PBAT biodegradation study but did not allude to their presence on the PBAT film surface or potential contribution to biodegradation. The data in our study suggests that although certain bacterial species were in the soil and on the PBAT film surface, they were unlikely to be significantly contributing to PBAT biodegradation within 35 days.

As reported by Muroi [37], examination of Figure 14 suggest that fungi play a more dominant role in PBAT biodegradation under mesophilic conditions in soil compared to bacteria, as can be observed from diversity and abundance results for PBAT film, which is comparable to, or exceeding the levels found in the soil. Of particular interest were select Ascomycota species such as *Westerdykella* sp. (Ascomycota 2) which showed an abundance of more than 3 times greater on the PBAT film surface than in the soil, suggesting that it has a dominant role in PBAT biodegradation. *Hypocreales* sp. and other unidentified fungi belonging to the Ascomycota phylum (Ascomycota 7 and 15 respectively) showed an abundance at least equal to levels on PBAT film surfaces when compared to soil. The data also suggests that only selective taxa belonging to the Ascomycota phylum will assimilate PBAT within 35 days when it is buried in soil under outdoor mesophilic conditions.

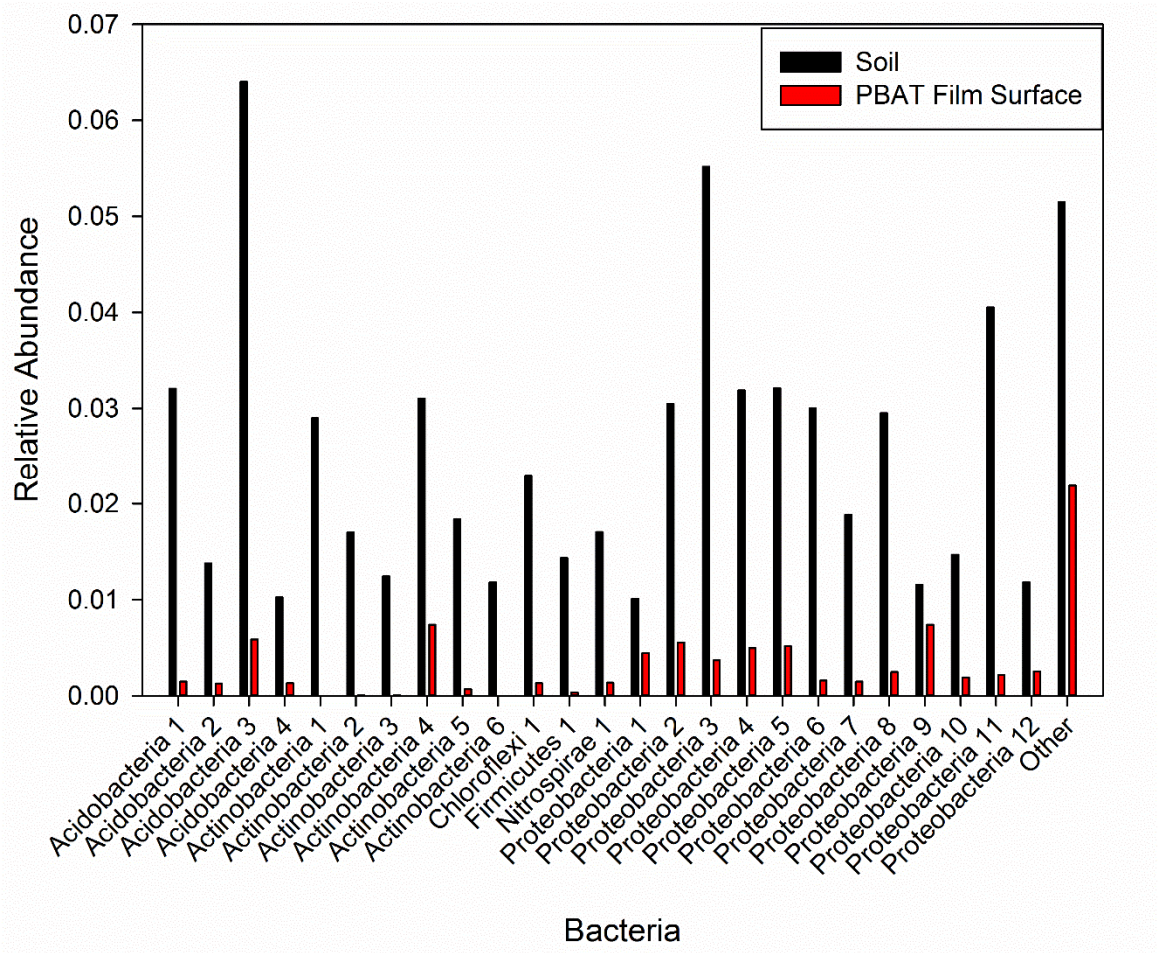


**Figure 13: Bacterial species diversity where the relative abundance is greater than 0.01 in the soil sample and on the film surface after 35 days burial at Pinjarra Hills, Qld, Australia.**

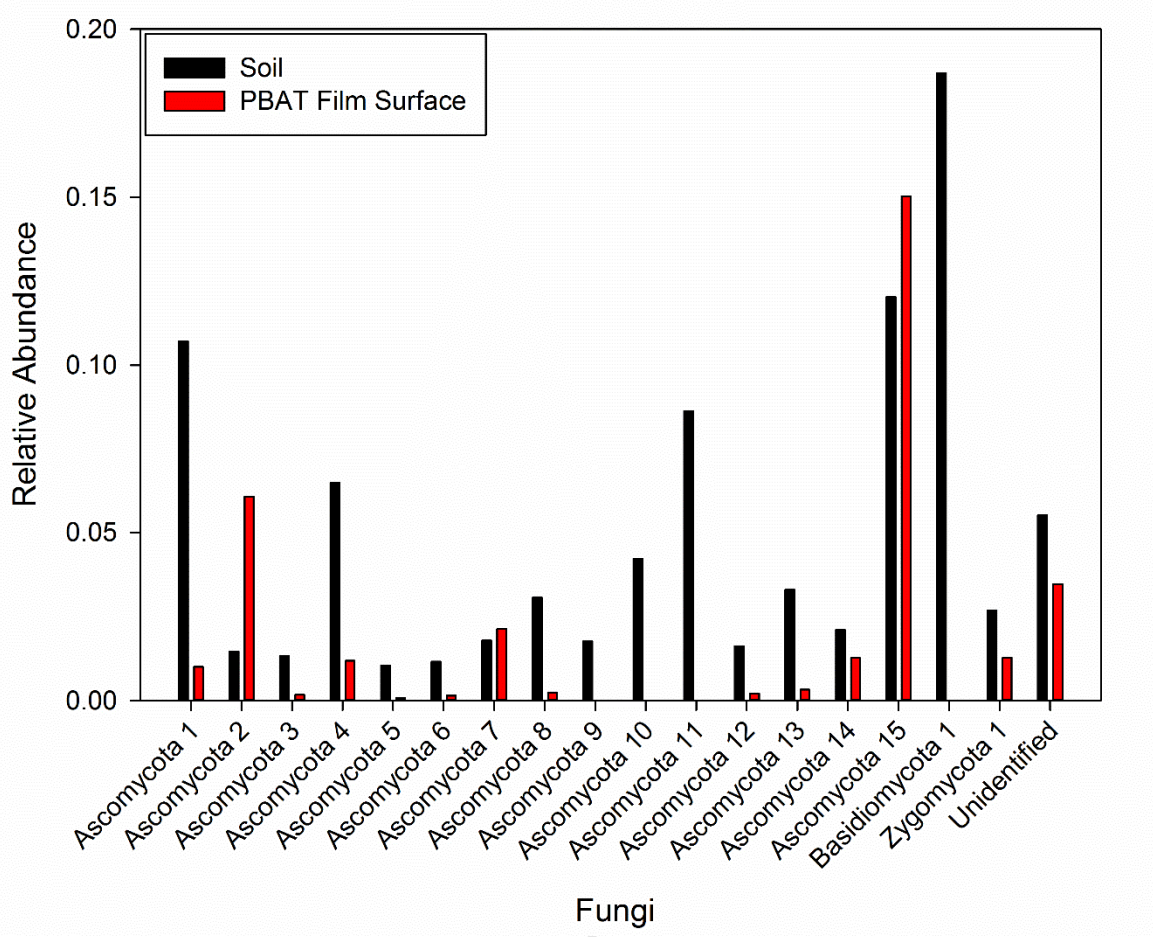


**Figure 14: Fungal species diversity where the relative abundance is greater than 0.01 in the soil sample and on the film surface after 35 days burial at Pinjarra Hills, Qld, Australia.**

The results from this study highlight the complexity in predicting the lifetime of PBAT film under mesophilic soil burial conditions under controlled laboratory conditions or outdoors, with differences in PBAT lifetime to failure being strongly influenced by film surface morphology as a result of fungi activity (particularly from select species from the Ascomycota phylum).

### 3.4 Above-ground degradation of PBAT

Although the biodegradation behaviour of PBAT buried in soil is a critical factor in determining performance and lifetimes of agricultural crop propagation film, the timing of the loss of mechanical properties of the PBAT above the emerging crop is also critical as shown by Figure 1 and discussion in Section 1.1. The degradation of this part of the film is strongly influenced by UV exposure rather than microbial events, although hydrolysis may expect to be a contributing factor to the strength loss with time depending on the water exposure and relative humidity in the confined environment under the canopy.

#### 3.4.1 Accelerated UV ageing of PBAT

To study the effect of moisture on the UV degradation of PBAT film, an experiment was undertaken where films were placed over Petri dishes that were filled with water or left empty and aged in a Q-Sun xenon-arc solar simulator (Section 2.2.1) and periodically tested by manually applying a small stress normal to the film plane. The first indication of mechanical failure under the applied stress was splitting of the film in the machine direction. The time to splitting was found to be faster over water than over air: 23.3±0.9 days of exposure for samples over water compared to 36±5.9 days of exposure over empty Petri dishes. These data show that condensed moisture, as would be present in agricultural film, significantly affects the rate of property loss. Likely routes are the hydrolysis of oxidation products such as anhydrides, and thermally driven hydrolysis of the polyester structure.

For experiments conducted in the dark at 60°C and 100% relative humidity, where moisture was observed to condense on the surfaces of the films, splitting was not observed, with failure (embrittlement) observed through multidirectional fracture of the films under a small applied stress. Embrittlement occurred after 50±4 days under these conditions. Comparatively, during simulated solar exposure (Q-Sun), equivalent, but heterogeneous, embrittlement behaviour was observed after 45 ± 1 days ageing in dry conditions at a lower average temperature (52°C), which shows that there is a strong influence of UV on the degradation rate of PBAT film.

The photo-degradation behaviour of PBAT has been studied by others [39-42] and it has been found that crosslinking occurs during photo-irradiation. The degree of crosslinking has been found to be affected by the aromatic content in the PBAT, where copolymers with higher aromatic content show a greater degree of crosslinking during irradiation. In one study [39], biodegradation tests under composting conditions showed that the mineralisation rate as measured by carbon dioxide production was not affected by the degree of crosslinking or photo-oxidation; instead, it was affected by the specific surface area of the polymer film samples. In contrast, a separate study by Kijchavengkul et al. [40] found that the degree of crosslinking in PBAT copolymers after photo-degradation did affect the subsequent rate of biodegradation in compost. However, their conclusion was drawn from the overall degree of mineralisation to carbon dioxide after a certain period of time, where the rate of carbon

dioxide production as a function of composting time showed more complex behaviour. Both of these studies indicate that (micro)-structural evolution with UV ageing may influence subsequent biodegradation rates of PBAT. However, UV exposure in both cases was undertaken in the absence of condensed moisture. Under most climatic and usage conditions, agricultural crop propagation film will have a layer of condensed water on the underside of the UV-exposed portion of the film, so the effect of moisture is a necessary area of study for determining the above-ground lifetimes of PBAT agricultural films.

### 3.4.2 IR Spectroscopic studies of UV ageing of PBAT film

The UV-exposed films were analysed via FTIR (Figure 15, Figure 16, Figure 18 and Figure 19). There is a large range of products that can be formed during photo-oxidation of aromatic (co)polyesters, which leads to the ability to monitor the degree of oxidation in several spectral regions. A range of carbonyl-containing species formed on oxidation generally leads to broadening of the initial ester band, with aliphatic and aromatic carboxylic acids, aldehydes, anhydrides and peresters being identified in photodegraded PET and other terephthalate copolymers, see Scheme 1. Here, the FTIR-ATR degree of oxidation has been expressed as an “anhydride/perester index” based on the peak height at 1785 $cm^{-1}$ (seen as a wing of the main carbonyl band from the initial ester groups) compared to the CH stretching peak area between 3045 and 2720 $cm^{-1}$, which has been used as an internal standard. The band at 1785 $cm^{-1}$ provides a point of distinction from the convoluted mixture of spectral bands that result from the other carbonyl species formed upon degradation.

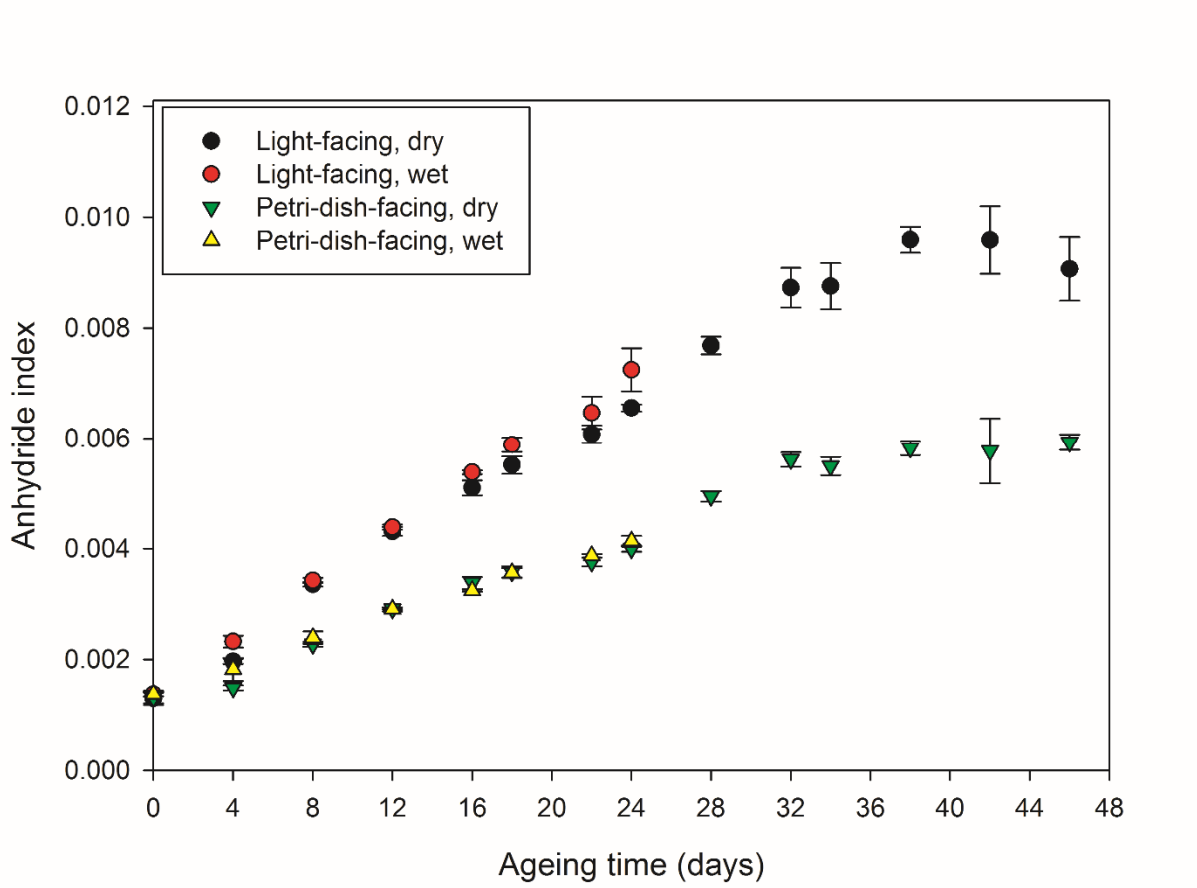


**Figure 15: FTIR-ATR spectral data for anhydride/perester formation on the light-facing and Petri-dish-facing surfaces of Q-Sun-aged PBAT films aged over air (dry) and aged over water (wet).**

Surprisingly, given the observation in the previous section that the time to splitting of the film was reduced from 36 days in air to 23 days over water, it was found that there were only very slight differences between oxidation rates of PBAT over air or over water. The most distinct difference shown in Figure 15 is between the light-facing and Petri-dish-facing surfaces of the PBAT samples. The light-facing surfaces showed greater degrees of oxidation than the Petri-dish-facing surfaces, suggesting that there is a screening effect by the (oxidised) PBAT. This is consistent with what has been observed for PET and another terephthalate copolymer [43], where the degree of the effect was found to be related to the concentration of terephthalate chromophores in the copolymer and is a result of UV absorption (see Figure 22 for the UV-Vis spectra for PBAT before and after ageing).

A subtle difference in the degradation of the dry and wet samples is evident in the rate of increase of the anhydride/perester index for the light-facing surfaces. The wet samples showed a slightly higher rate of oxidation than the dry samples, which may be influenced by parameters discussed in Section 3.1, such as: reflection of UV from condensed moisture droplets on the underside of the film. However, there was no discernible difference between the rates of oxidation for the wet and dry

samples on the Petri-dish-facing surfaces. At this surface, which is in contact with water, moisture may play a role in reducing the concentration of anhydride and perester groups via hydrolysis. In bulk analysis of the films via transmission FTIR (Figure 16), the absorbance at 1785 $cm^{-1}$ for the wet samples showed a slightly lower rate of increase with ageing time compared to the dry samples. This may be due to hydrolysis of the anhydride and perester groups over time as proposed above, and suggests that the slightly higher anhydride/perester index seen on the light-facing surfaces of wet samples is outweighed by hydrolysis throughout the bulk of the material. Ultimately, hydrolysis of anhydrides and peresters will lead to chain scission (Scheme 1) and may help to explain the earlier time to splitting seen for wet samples compared to dry samples.

In addition to monitoring degradation of the PBAT samples at 1785 $cm^{-1}$, changes in absorbance at 1650 $cm^{-1}$ and the broad band centred around 3245 $cm^{-1}$ were monitored throughout ageing. See Figure 17 for FTIR spectra, showing generic changes in these bands with ageing, and Figure 18 and Figure 19 for the change in absorbance during ageing. These infrared bands correspond to double bonds and carboxyl groups, respectively, with the formation of these products being consistent with those observed during UV-induced degradation of PET and other terephthalate copolymers as shown in Scheme 1 [43, 44]. At 1650 $cm^{-1}$, there are negligible differences between wet and dry samples, which suggests that the Norrish type II reaction that leads to the formation of double bonds is not affected by the presence of moisture. For the broad band centred around 3245 $cm^{-1}$, there are also only very slight differences in the rates of growth over time. Considering that the hydrolysis of an anhydride or perester should lead to the formation of carboxyl groups, it is unclear why the same proportional difference between wet and dry samples monitored at 1785 $cm^{-1}$ is not seen at 3245 $cm^{-1}$. Overall, there are only subtle differences in the IR spectra from wet and dry samples and complementary techniques may be required to understand the reasons for the observed differences in embrittlement times.

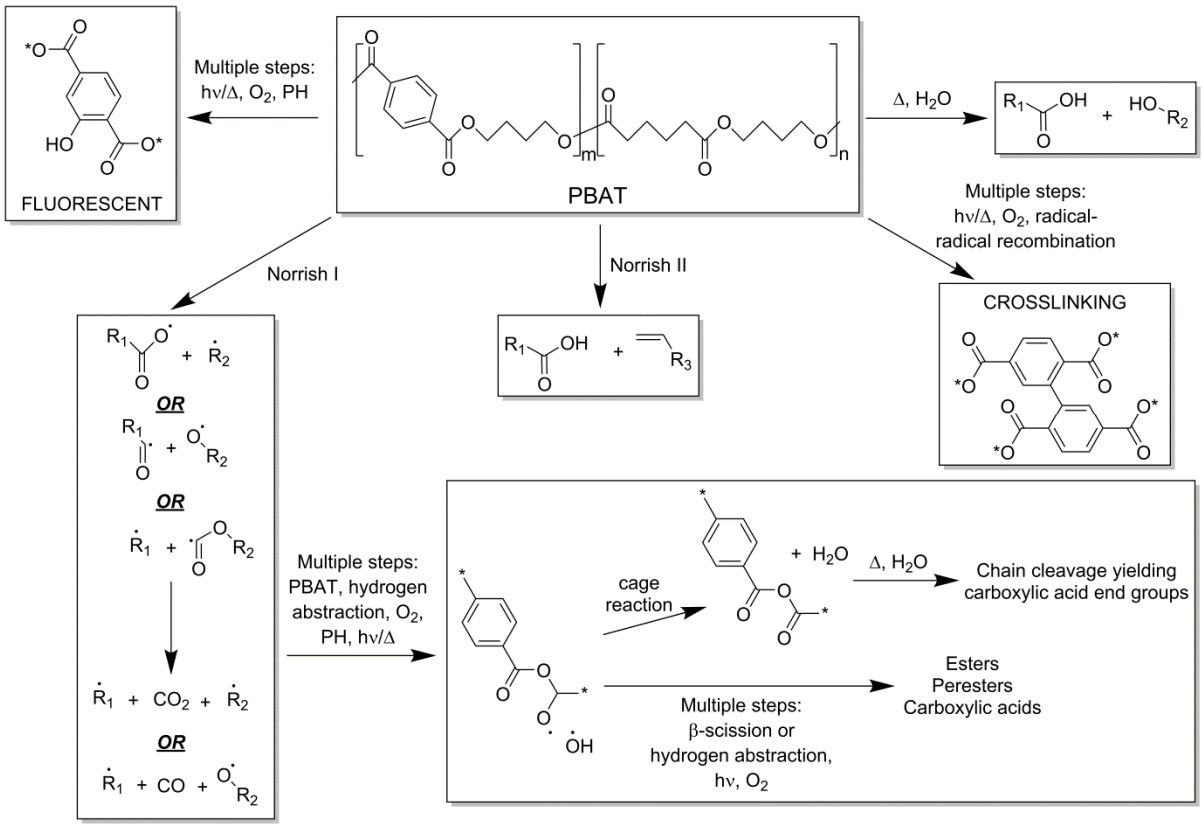


**Scheme 1: A summary of the products that may be formed on photo-oxidation of PBAT, based on mechanisms proposed for PET and other terephthalate copolymers [43-45]. Also shown is thermally-driven hydrolysis in the presence of moisture, which may occur when PBAT is aged in a moist environment.**

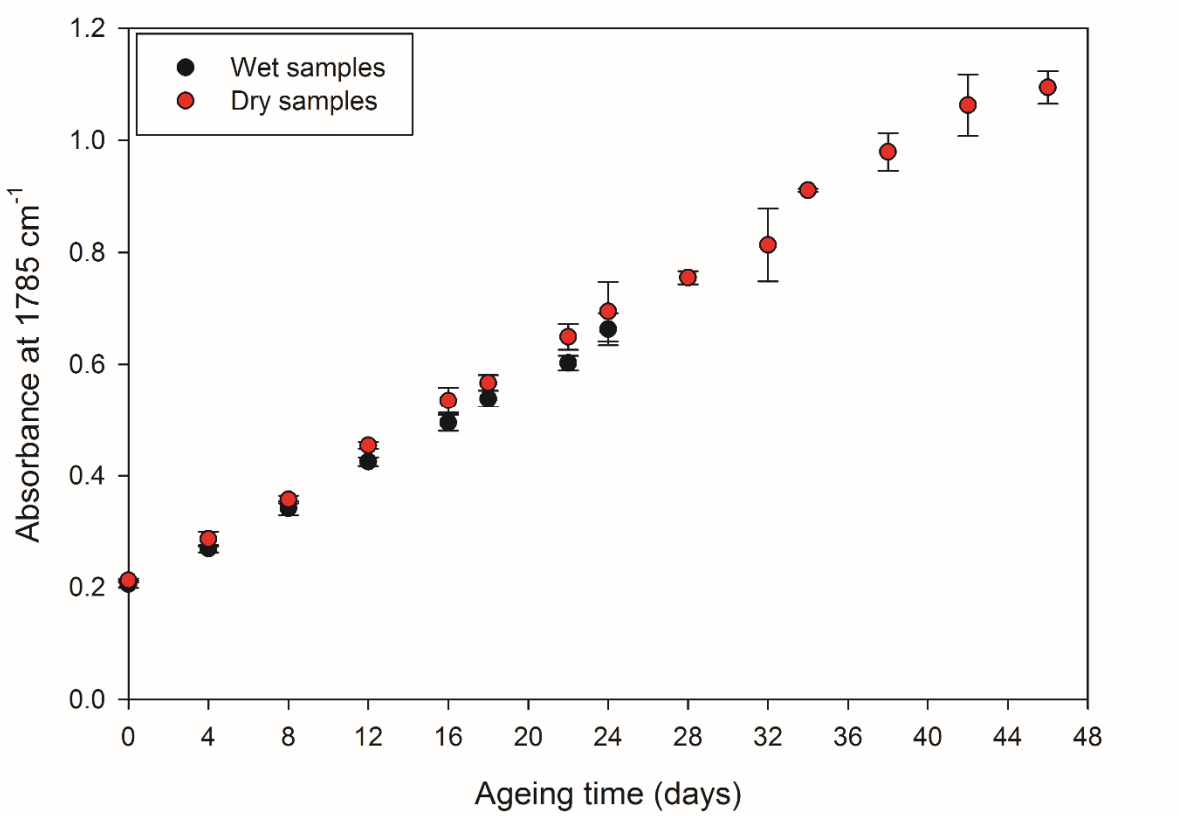


**Figure 16: FTIR transmission spectral data for bulk anhydride formation in Q-Sun-aged PBAT films aged over air (dry samples) and aged over water (wet samples).**

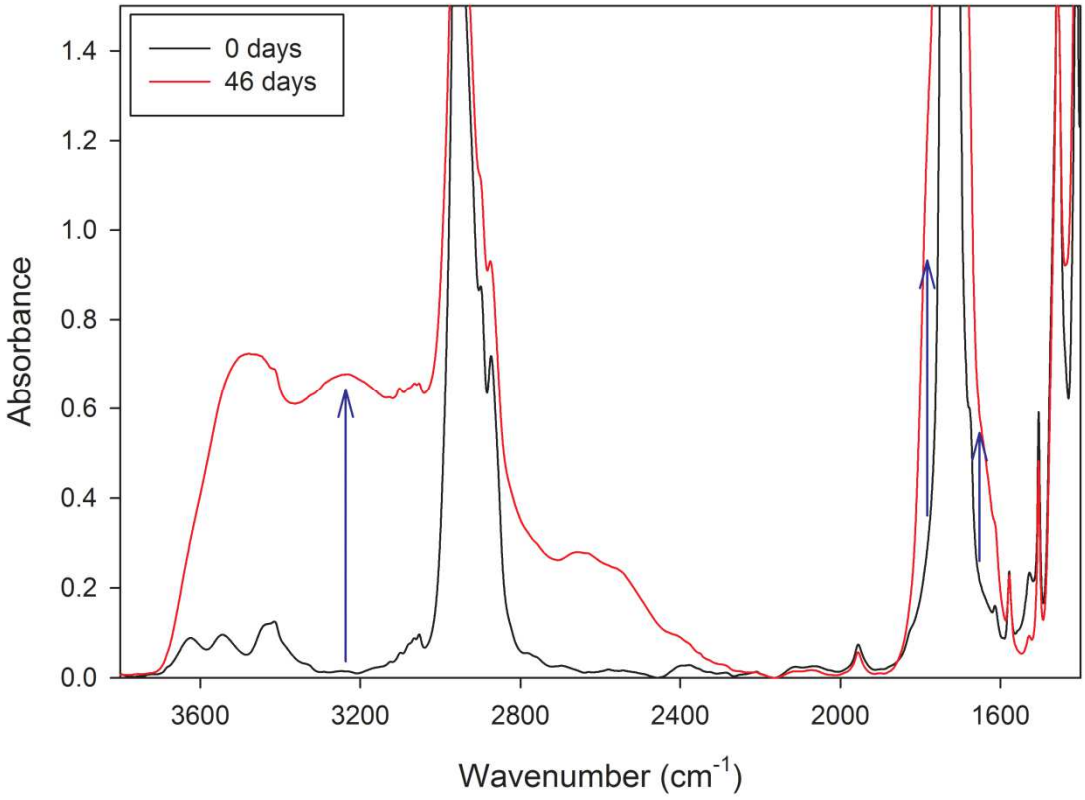


**Figure 17: FTIR transmission spectra for Q-Sun-aged PBAT films before and after ageing over air (dry samples) for 46 days, showing changes in absorbance at 1650 $cm^{-1}$, 1785 $cm^{-1}$ and the broad band centred around 3245 $cm^{-1}$ (blue arrows).**

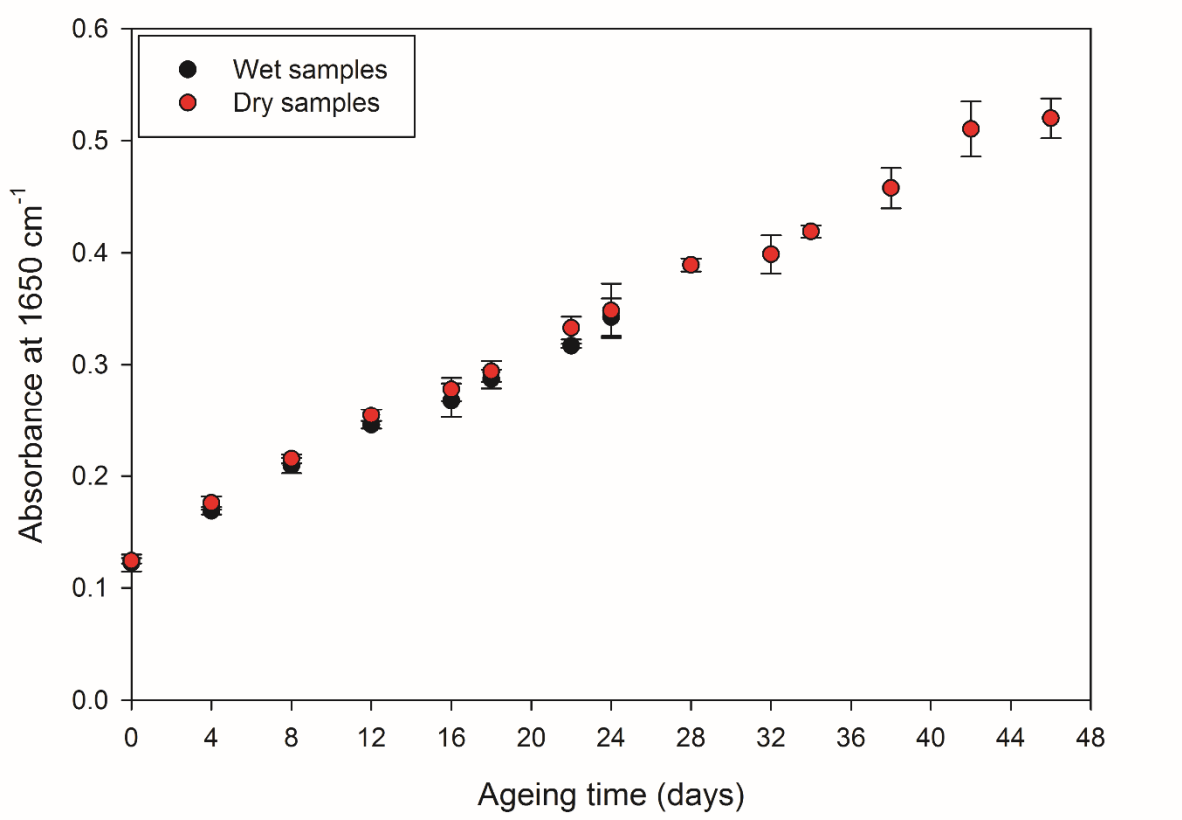


**Figure 18: FTIR transmission spectral data for bulk formation of double bonds in Q-Sun-aged PBAT films aged over air (dry samples) and aged over water (wet samples).**

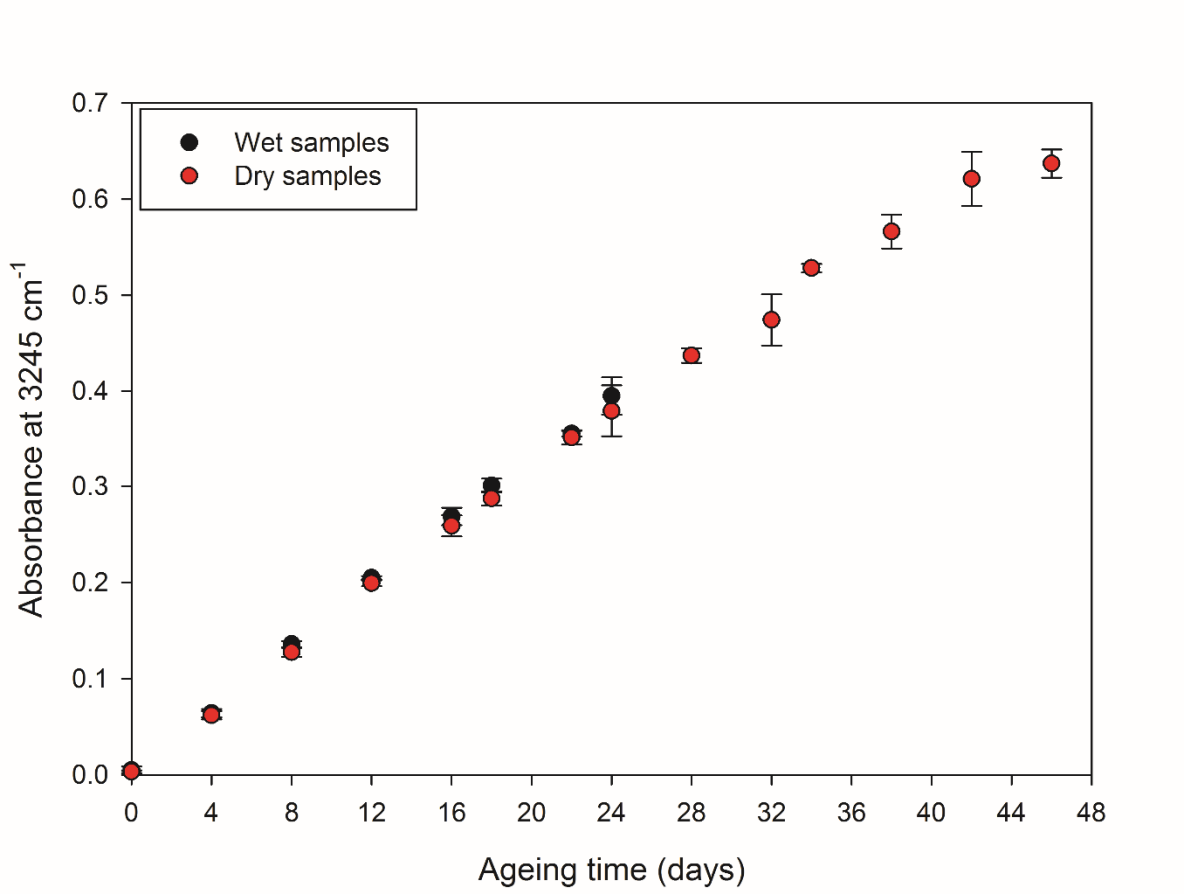


**Figure 19: FTIR transmission spectral data for bulk formation of carboxyl groups in Q-Sun-aged PBAT films aged over air (dry samples) and aged over water (wet samples).**

### 3.4.3 Analysis of UV-aged PBAT samples via fluorescence methods

UV black-light inspection (predominantly 365 nm) of PBAT films after ageing in a QUV apparatus for ten days showed that they were strongly fluorescent, compared to an unaged PBAT film, which was not fluorescent. Equivalent UV dose rates below 340 nm were used in the QUV and Q-Sun ageing experiments. Images were taken and examples are shown in Figure 20.

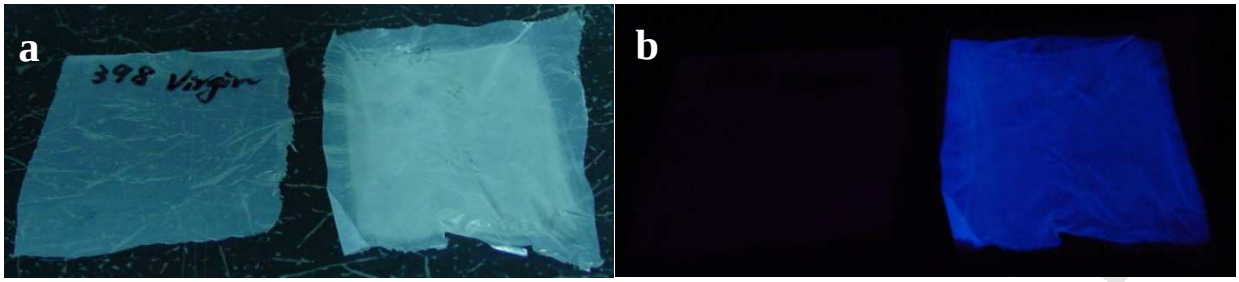


**Figure 20: a: Room light image - Unaged PBAT film sample (left) and QUV-aged PBAT sample (right). b: UV light (1/25 sec. exposure) – Unaged PBAT film sample (left) and QUV-aged PBAT sample (right). Note that the border (which was not exposed to UV during ageing) of the QUV-aged sample did not fluoresce.**

The room-light image of the UV-irradiated PBAT film in Figure 20a also shows that the section irradiated is obvious from the weak fluorescence and the non-fluorescent border. Fluorescence and UV-Visible spectra were also measured (Figure 21 and Figure 22, respectively). The increase in fluorescence observed between unaged and aged samples may be used as another method for indexing degradation in these materials and has the advantage that it is non-contact and may be made portable for field studies. The observed fluorescence emission is analogous to that observed for photodegraded PET and other terephthalate copolymers [45, 46], where the formation of a fluorescent hydroxylated terephthalate species has been observed (see Scheme 1 for a generic chemical structure).

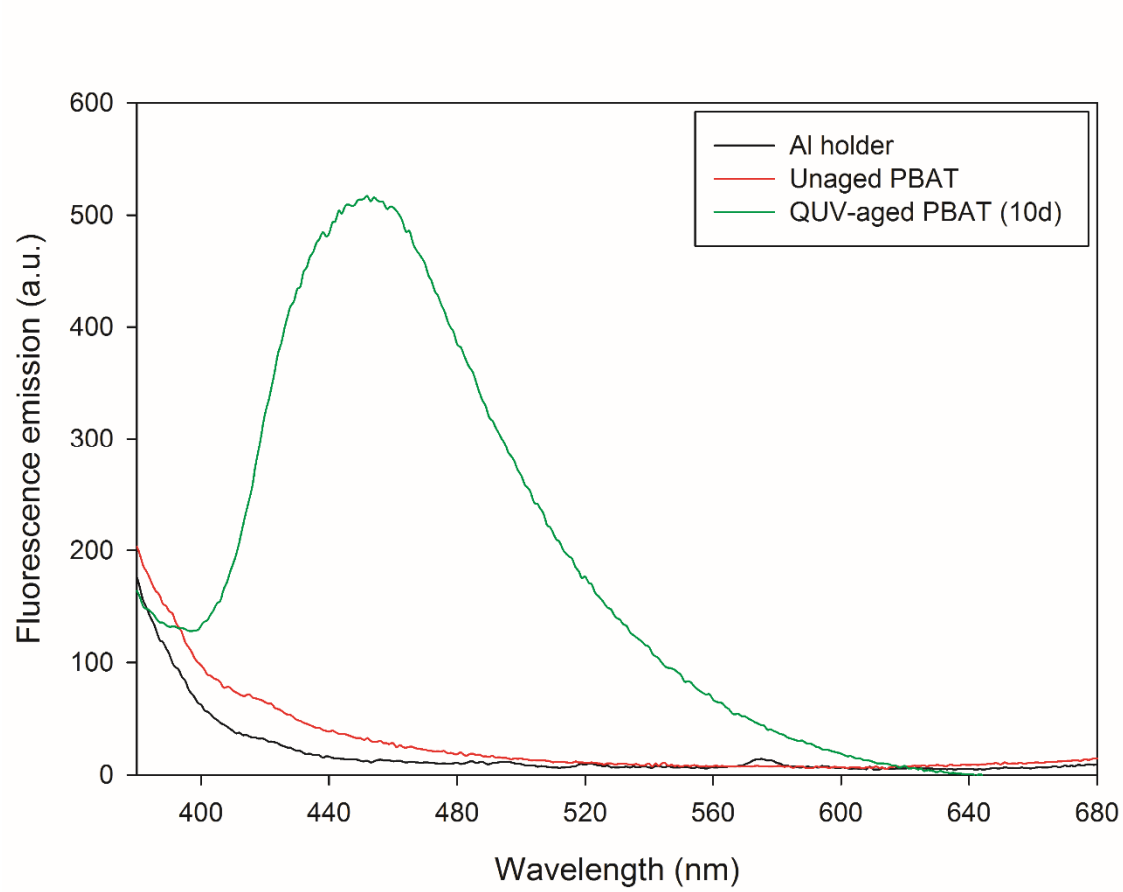


**Figure 21: Fluorescence emission spectra from PBAT samples (unaged and QUV-aged for 10 days), as well as an aluminium holder that was used as a support for the films during the measurements. The spectra were measured using a fibre optic probe with a 45° take-off head. Excitation was at 365 nm.**

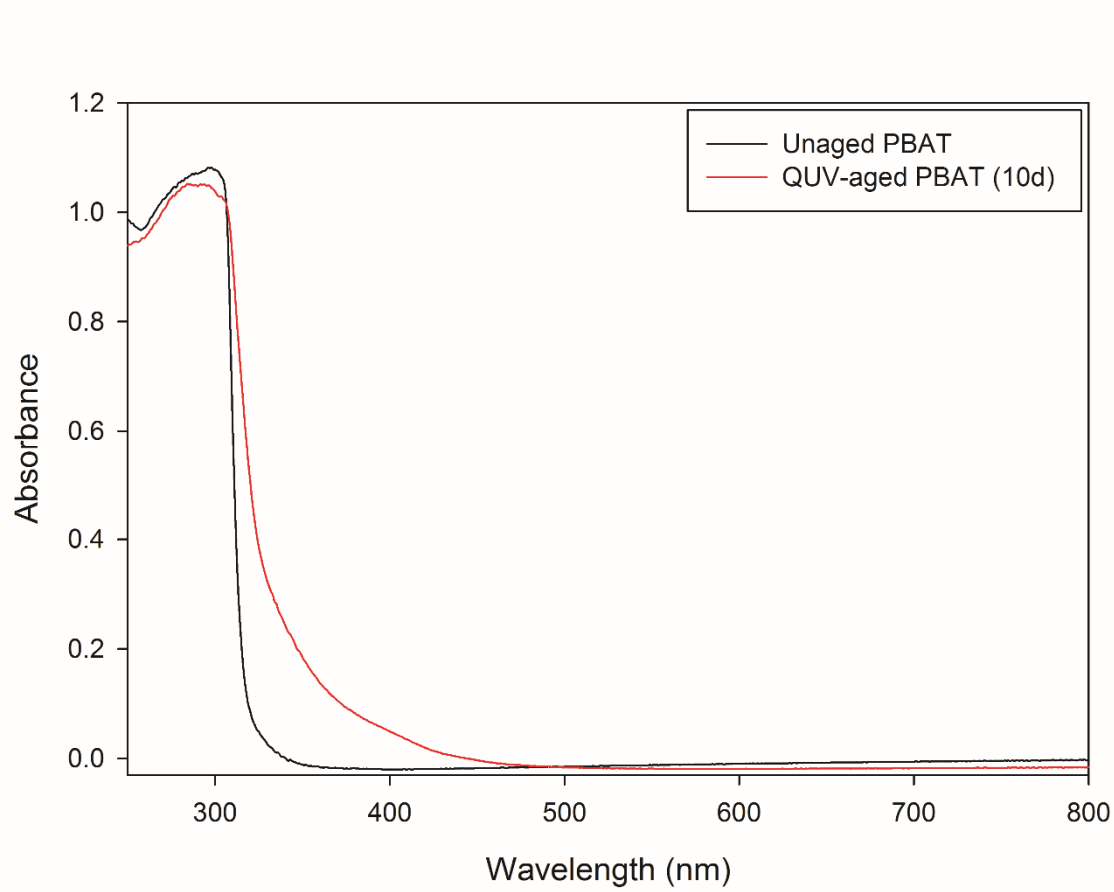


**Figure 22: UV-Vis integrating sphere measurements from PBAT samples (unaged and QUV-aged for 10 days). These spectra show increases in absorbance for the aged sample in the UV and blue regions of the spectrum, which is consistent with yellowing of the material.**

Structural changes during UV exposure have been shown to influence the rate of subsequent biodegradation [39-42], so UV degradation has a critical influence on the ultimate lifetime of PBAT copolymers (i.e. during Stage 2 of Figure 2).

## 4.0 Conclusions

The total lifetime of a degradable polymer film when used for applications such as agriculture, packaging, etc. can be considered in two stages:

1. The useful mechanical lifetime where properties such as strength and toughness are maintained for sufficient time to fulfil its intended application after which degradation then commences and the polymer ultimately embrittles;
2. The ultimate fate of the embrittled polymer that involves bio-assimilation of the products of polymer degradation. This stage is often considered in legislative requirements for

biodegradation where the rate of carbon dioxide evolution is measured in the laboratory when the film is buried in soil or compost.

Only the time taken for Stage 1 has been considered in this study for both UV exposure and burial of an oxodegradable polyolefin (LLDPE + 1% P25) and a biodegradable polymer, PBAT.

From laboratory studies, the factors to consider for the outdoor lifetime of photo-sensitive oxodegradable polymers such as LLDPE + 1% nano-titania (as the anatase/rutile mixed phase P25) were expected to be just UV dose and temperature. However, when this was translated to the field with the film exposed in the confined environment above the soil, the factors affecting degradation rate include soil parameters such as moisture and organic material content. In addition to the physical effects of the soil such as reflectivity and moisture beading on the reverse face of the film, the possibility of generation of reactive oxygen species from soil cannot be excluded. This provides a significant challenge in translating from laboratory accelerated ageing studies to the prediction of the useful mechanical lifetime when exposed outdoors as the rate of degradation becomes site specific.

In the particular application of the oxodegradable films for cropping, the edges of the film are buried and a strategy of pre-irradiation with UV-C (254 nm) increased the concentration of peroxides and/or hydroperoxides in the films as detected by temperature-ramped chemiluminescence under nitrogen. Oven ageing at 100% RH and 60°C produced accelerated embrittlement of both LLDPE and LLDPE + 1% P25 pre-irradiated films. However, the observed extent of degradation was predicted to not meet the application demands of embrittlement of the film within 6 months of burial, assuming an acceleration factor of ~16 from the test temperature to soil temperature. This was confirmed from a 6-month field trial and it was concluded that this strategy would not meet the demands of cropping film degradation below the ground.

The factors controlling the loss of properties of a biodegradable PBAT clear film when buried have been studied at a field site and also in the laboratory with well-characterized soil. The rate of degradation in the field was much higher than for the same period in the laboratory, possibly reflecting the higher average temperature and moisture content. The elongation-at-break fell from 900% to 70% in one month in the field while similar changes required 6 months in the laboratory. There was little change in $\bar{M}_n$ for embrittlement in the field while in the laboratory there was the start of a decrease in $\bar{M}_n$ at embrittlement although this took a much longer time. This suggests that the loss of mechanical properties was not linked to a bulk property such as change in $\bar{M}_n$ but rather to surface changes as seen by SEM. The morphology changes observed were different with the laboratory sample having localized extensive degradation leading to holes while the sample buried outdoors had an extensive network of surface cracks. Embrittlement in the laboratory sample did not occur until these holes were interconnected which required a total loss of 6.5% mass while the outdoor sample

lost only 2% mass at embrittlement. Such observations are consistent with the fracture toughness being controlled by the size and depth of the cracks rather than change in $\bar{M}_n$ or loss of mass. This suggests that even in thin films, enzyme-mediated hydrolysis of PBAT is surface controlled. Heating of the PBAT in an oven at 60°C for 100 days (equivalent to over 12 months at 40°C, the highest soil temperature) showed the surface of the film was smooth and there was no crack formation indicating that the changes in morphology are microbiological in origin.

DNA analysis of the soil around the buried films after 35 days ageing outdoors showed fungi play a more dominant role in PBAT biodegradation under mesophilic conditions in soil compared to bacteria. The accelerated degradation when buried outdoors compared to the laboratory may reflect the greater diversity in the fungal population which is lost under the controlled temperature and moisture conditions in the laboratory. This has some implications when the certification of biodegradable polymers is focussed on carbon dioxide evolution under controlled laboratory conditions but this is important for the time for Stage 2 of the degradation pathway rather than the Stage 1 processes that result in strength loss and embrittlement.

UV degradation of PBAT film is primarily controlled by the photochemistry of the terephthalate moiety in the polymer and the development of fluorescence is a useful indicator of the extent of photo-degradation. Interestingly the extent of photo-product formation with time of UV exposure did not depend on whether the film was exposed over water or over air, but there were strength losses suggesting that hydrolysis was involved in the degradation pathway under the conditions studied.

The practical solution to the requirements of degradable cropping film have yet to be achieved as the ideal system would incorporate the above-ground performance of polyolefins (low cost, mechanical properties and lifetime control achievable with suitable additives) and the below-ground performance of PBAT (biodegradability and good mechanical properties but at a high cost). The future challenge is to achieve this with a novel blend that exploits the best properties of each polymer.

## 5.0 Acknowledgments

The authors would like to thank and acknowledge the support of the Cooperative Research Centre for Polymers and Integrated Packaging for the financial support of this research. This work would not have been possible without the contributions of the following to sample preparation and testing: Dr Chun-Liang Yeh, Mr Michael Murphy, Mr John Milne, Dr Greg Cash and Dr Jorja Cork. We thank Professor Graeme George for editorial assistance and Dr Jozef Rychly and Dr Lyda Rychla for their contribution to the Chemiluminescence study.

## 6.0 References

[1] Global agriculture towards 2050 FAO. http://www.fao.org/fileadmin/templates/wsfs/docs/Issues_papers/HLEF2050_Global_Agriculture.pdf. (Accessed 20th March 2017).
[2] R. Kingwell, L. Anderton, N. Islam, V. Xayavong, A. Wardell-Johnson, D. Feldman, J. Speijers. Broadacre farmers adapting to a changing climate, National Climate Change Adaptation Research Facility, Gold Coast, 2013.
[3] Bowman & Associates Pty Ltd, The Gascoyne Development Commission. Biodegradable alternatives and recycling opportunities for agricultural mulch film and drip irrigation tape for the Gascoyne fruit and vegetable grower, 2009. http://www.wasteauthority.wa.gov.au/media/files/grant_projects/GDC_biodegradable_final_report_SWIS2008.pdf. (Accessed 20th March 2017).
[4] N. Thomas, J. Clarke, A. McLauchlin, S. Patrick. EV0422 Assessing the Environmental Impacts of Oxo-degradable Plastics Across Their Life Cycle, Loughborough University, London, 2010. http://randd.defra.gov.uk/Default.aspx?Module=More&Location=None&ProjectID=16263. (20th March 2017).
[5] B. Laycock, M. Nikolic, J. Colwell, E. Gauthier, P. Halley, S. Bottle, G. George, Lifetime prediction of biodegradable polymers, Prog. Polym. Sci. (2017) *Accepted February 2017, in press*.
[6] G. Scott, D.M. Wiles, Programmed-life plastics from polyolefins: a new look at sustainability, Biomacromolecules 2(3) (2001) 615-622.
[7] M.C. Celina, Review of polymer oxidation and its relationship with materials performance and lifetime prediction, Polym. Degrad. Stab. 98(12) (2013) 2419-2429.
[8] J. Verdu, Oxidative Ageing of Polymers, John Wiley and Sons, London, UK, 2012.
[9] I. Blakey, B. Goss, G. George, Chemiluminescence as a probe of polymer oxidation, Aust. J. Chem. 59(8) (2006) 485-498.
[10] G.A. George, M. Celina, Homogeneous and heterogeneous oxidation of polypropylene, in: H.S. Hamid (Ed.), Handbook of Polymer Degradation, Second Edition, Marcel Dekker, New York, 2000, pp. 277-314.
[11] M. Nikolic, E. Gauthier, J. Colwell, B. Laycock, C.-L. Yeh, G. Cash, P. Halley, S. Bottle, G.A. George, Chapter 7: Real-world factors that impact polyolefin lifetimes, in: J.P. Lewicki, G. Overturf (Eds.), Lifetimes and Compatibility of Synthetic Polymers, Scrivener Publishing LLC, Beverly, MA 2017, p. *in press*.
[12] A.C. Vieira, J.C. Vieira, J.M. Ferra, F.D. Magalhaes, R.M. Guedes, A.T. Marques, Mechanical study of PLA-PCL fibers during in vitro degradation, J. Mech. Behav. Biomed. Mater. 4(3) (2011) 451-460.
[13] Australian Government Bureau of Meteorology. http://www.bom.gov.au/. (Accessed 16th March 2017).
[14] Australian Radiation Protection and Nuclear Safety Agency. http://www.arpansa.gov.au/. (Accessed 17th March 2017).
[15] G.A. George, P. Johnstone, J. Warner, P. Halley, B. Laycock, S. Gardi, C. Pasti, G. Schlingloff. Degradable Polymeric Films WO2009021270 A1 (2009).
[16] B. Ohtani, S. Adzuma, S.-i. Nishimoto, T. Kagiya, Photocatalytic degradation of polyethylene film by incorporated extra-fine particles of titanium dioxide, Polym. Degrad. Stab. 35(1) (1992) 53-60.
[17] E. Gauthier, M. Nikolić, R. Truss, B. Laycock, P. Halley, Effect of soil environment on the photo-degradation of polyethylene films, J. Appl. Polym. Sci. 132(39) (2015) 1-10.
[18] A.F. McKinlay, B.L. Differy, A reference action spectrum for ultraviolet induced erythema in human skin, in: W.F. Passchier, B.F.M. Bosnjakovic (Eds.), Human Exposure to Ultraviolet Radiation: Risks and Regulations, Elsevier Science, Amsterdam, 1987, pp. 83-87.
[19] X. Yan, T. Ohno, K. Nishijima, R. Abe, B. Ohtani, Is methylene blue an appropriate substrate for a photocatalytic activity test? A study with visible-light responsive titania, Chem. Phys. Lett. 429(4-6) (2006) 606-610.

[20] M. Nikolic, E. Gauthier, K. George, G. Cash, M.D. de Jonge, D.L. Howard, D. Paterson, B. Laycock, P.J. Halley, G. George, Antagonism between transition metal pro-oxidants in polyethylene films, Polym. Degrad. Stab. 97(7) (2012) 1178-1188.
[21] K. Jacobson, P. Eriksson, T. Reitberger, B. Stenberg, Chemiluminescence as a tool for polyolefin oxidation studies, in: A.-C. Albertsson (Ed.), Long Term Properties of Polyolefins, Springer Berlin Heidelberg, Berlin, Heidelberg, 2004, pp. 151-176.
[22] X. Tang, S. Alavi, Recent advances in starch, polyvinyl alcohol based polymer blends, nanocomposites and their biodegradability, Carbohydr. Polym. 85(1) (2011) 7-16.
[23] W. Amass, A. Amass, B. Tighe, A review of biodegradable polymers: uses, current developments in the synthesis and characterization of biodegradable polyesters, blends of biodegradable polymers and recent advances in biodegradation studies, Polym. Int. 47(2) (1998) 89-144.
[24] D. Demirgöz, C. Elvira, J.F. Mano, A.M. Cunha, E. Piskin, R.L. Reis, Chemical modification of starch based biodegradable polymeric blends: effects on water uptake, degradation behaviour and mechanical properties, Polym. Degrad. Stab. 70(2) (2000) 161-170.
[25] L. Averous, L. Moro, P. Dole, C. Fringant, Properties of thermoplastic blends: starch–polycaprolactone, Polymer 41(11) (2000) 4157-4167.
[26] R.N. Tharanathan, Biodegradable films and composite coatings: past, present and future, Trends Food Sci. Technol. 14(3) (2003) 71-78.
[27] J.K. Pandey, K. Raghunatha Reddy, A. Pratheep Kumar, R.P. Singh, An overview on the degradability of polymer nanocomposites, Polym. Degrad. Stab. 88(2) (2005) 234-250.
[28] K.O. Siegenthaler, A. Künkel, G. Skupin, M. Yamamoto, Ecoflex® and Ecovio®: Biodegradable, performance-enabling plastics, 2012, pp. 91-136.
[29] Z. Saadi, G. Cesar, H. Bewa, L. Benguigui, Fungal degradation of poly(butylene adipate-co-terephthalate) in soil and in compost, J. Polym. Environ. 21(4) (2013) 893-901.
[30] T. Kijchavengkul, R. Auras, M. Rubino, S. Selke, M. Ngouajio, R.T. Fernandez, Biodegradation and hydrolysis rate of aliphatic aromatic polyester, Polym. Degrad. Stab. 95(12) (2010) 2641-2647.
[31] U. Witt, T. Einig, M. Yamamoto, I. Kleeberg, W.D. Deckwer, R.J. Muller, Biodegradation of aliphatic-aromatic copolyesters: evaluation of the final biodegradability and ecotoxicological impact of degradation intermediates, Chemosphere 44(2) (2001) 289-299.
[32] K.-i. Kasuya, N. Ishii, Y. Inoue, K. Yazawa, T. Tagaya, T. Yotsumoto, J.-i. Kazahaya, D. Nagai, Characterization of a mesophilic aliphatic–aromatic copolyester-degrading fungus, Polym. Degrad. Stab. 94(8) (2009) 1190-1196.
[33] F. Trinh Tan, D.G. Cooper, M. Marić, J.A. Nicell, Biodegradation of a synthetic co-polyester by aerobic mesophilic microorganisms, Polym. Degrad. Stab. 93(8) (2008) 1479-1485.
[34] S.J. Wang, L. Copeland, Effect of acid hydrolysis on starch structure and functionality: a review, Crit. Rev. Food Sci. Nutr. 55(8) (2015) 1079-1095.
[35] R. Muthuraj, M. Misra, A.K. Mohanty, Hydrolytic degradation of biodegradable polyesters under simulated environmental conditions, J. Appl. Polym. Sci. 132(27) (2015) n/a-n/a.
[36] P. Rychter, M. Kawalec, M. Sobota, P. Kurcok, M. Kowalczuk, Study of aliphatic-aromatic copolyester degradation in sandy soil and its ecotoxicological impact, Biomacromolecules 11(4) (2010) 839-847.
[37] F. Muroi, Y. Tachibana, Y. Kobayashi, T. Sakurai, K.-i. Kasuya, Influences of poly(butylene adipate-co-terephthalate) on soil microbiota and plant growth, Polym. Degrad. Stab. 129 (2016) 338-346.
[38] H. Wang, D. Wei, A. Zheng, H. Xiao, Soil burial biodegradation of antimicrobial biodegradable PBAT films, Polym. Degrad. Stab. 116 (2015) 14-22.
[39] P. Stloukal, V. Verney, S. Commereuc, J. Rychly, L. Matisova-Rychla, V. Pis, M. Koutny, Assessment of the interrelation between photooxidation and biodegradation of selected polyesters after artificial weathering, Chemosphere 88(10) (2012) 1214-1219.
[40] T. Kijchavengkul, R. Auras, M. Rubino, M. Ngouajio, R.T. Fernandez, Assessment of aliphatic-aromatic copolyester biodegradable mulch films. Part II: Laboratory simulated conditions, Chemosphere 71(9) (2008) 1607-1616.

[41] T. Kijchavengkul, R. Auras, M. Rubino, M. Ngouajio, R.T. Fernandez, Assessment of aliphatic-aromatic copolyester biodegradable mulch films. Part I: field study, Chemosphere 71(5) (2008) 942-53.
[42] S. Commereuc, H. Askanian, V. Verney, A. Celli, P. Marchese, About durability of biodegradable polymers: structure/degradability relationships, Macromolecular Symposia 296(1) (2010) 378-387.
[43] T. Grossetete, A. Rivaton, J.L. Gardette, C.E. Hoyle, M. Ziemer, D.R. Fagerburg, H. Clauberg, Photochemical degradation of poly(ethylene terephthalate)-modified copolymer, Polymer 41 (2000) 3541-3554.
[44] A. Rivaton, Photochemistry of poly(butyleneterephthalate): 2-Identificiation of the IR-absorbing photooxidation products, Polym. Degrad. Stab. 41 (1993) 297-310.
[45] N.S. Allen, G. Rivalle, M. Edge, I. Roberts, D.R. Fagerburg, Characterisation and identification of fluorescent hydroxylated terephthalate species in the thermal and UV degradation of poly(ethylene-co-1,4-cyclohexanedimethylene terephthalate) (PECT), Polym. Degrad. Stab. 67 (2000) 325-334.
[46] G.J.M. Fechine, M.S. Rabello, R.M. Souto Maior, L.H. Catalani, Surface characterization of photodegraded poly(ethylene terephthalate). The effect of ultraviolet absorbers, Polymer 45(7) (2004) 2303-2308.
[47] J. Zhang, K. Kobert, T. Flouri, A. Stamatakis, PEAR: a fast and accurate Illumina Paired-End reAd mergeR, Bioinformatics 30(5) (2014) 614-620.
[48] K.J. Caporaso JG, Stombaugh J, Bittinger K, Bushman FD, Costello EK,Fierer N, Peña AG, Goodrich JK, Gordon JI, Huttley GA, Kelley ST, Knights D,Koenig JE, Ley RE, Lozupone CA, McDonald D, Muegge BD, Pirrung M, Reeder J, Sevinsky JR, Turnbaugh PJ, Walters WA, Widmann J, Yatsunenko T, Zaneveld J, Knight R., QIIME allows analysis of high-throughput community sequencing data, Nat. Methods 7(5) (2010) 335-6.
[49] R. Edgar, Search and clustering orders of magnitude faster than BLAST, Bioinformatics 26(19) (2010) 2460-1.
[50] H.B. Edgar RC, Clemente JC, Quince C, Knight R., UCHIME improves sensitivity and speed of chimera detection, Bioinformatics 27(16) (2011) 2194-200.

# 7.0 Supplementary Information

## 7.1 Microbial DNA Isolation and Sequencing

Bacterial 16S rDNA and fungal Internal Transcribed Spacer (ITS) regions within the microbiota on the surface of buried PBAT film and the soil in the vicinity of the buried film (< 2mm from top of film surface) were assessed and compared for diversity and population after 35 days incubation at the outdoor weathering site. Immediately following collection, samples were placed in sterile tubes or sample bags, stored on dry ice during transit, followed by storage at -80°C until further use. A commercial laboratory, Australian Genome Research Facility (AGRF) performed the DNA isolation on both samples of soil and film using a DNeasy PowerLyzer PowerSoil Kit (MO BIO Laboratories, now a Qiagen Company) according to the specification of the supplier. Microbiota from the PBAT film surface were collected by cutting approximately 18 $cm^2$ of PBAT film into smaller pieces followed by washing and filtering with sterile water. Bacterial 16S rDNA and fungal Internal Transcribed Spacer (ITS) regions were amplified by Polymerase Chain Reaction (PCR) according to the Illumina metagenomics sequencing library preparation guide, using the Nextera Xt v2 dual direction indices to barcode each amplicon.

**Table S1: PCR amplicon targets used to characterize bacterial and fungal species.**

| | Bacteria | Fungi |
|---|---|---|
| Target | 27F-519R | ITS1F – ITS2 |
| Forward primer | AGAGTTTGATCMTGGCTCAG | CTTGGTCATTTAGAGGAAGTAA |
| Reverse primer | GWATTACCGCGGCKGCTG | GCTGCGTTCTTCATCGATGC |

The resulting amplicons were measured by florometry (Invitrogen Picogreen) and normalised. The eqimolar pool was then measured by qPCR (KAPA) followed by sequencing on the Illumina MiSeq (San Diego, CA, USA) with 2 x 300 base pairs paired-end chemistry.

Image analysis was performed in real time by the MiSeq Control Software (MCS) v2.5.0.5 and Real Time Analysis (RTA) v1.18.54, running on the instrument computer. RTA performed real-time base calling on the MiSeq instrument computer followed by the Illumina bcl2fastq 2.18.0.12 pipeline to generate the sequence data.

Paired-ends reads were assembled by aligning the forward and reverse reads using PEAR (Paired-End Read merger) [47] (version 0.9.5). Primers were identified and trimmed. Trimmed sequences were processed using Quantitative Insights into Microbial Ecology (QIIME 1.8) [48], USEARCH

(algorithms enabling sensitive local and global search of large sequence databases at exceptionally high speeds) [49, 50] (version 8.0.1623) and UPARSE software (a method for generating operational taxonomic unit clusters from next generation sequencing reads of marker 16S rDNA and fungal ITS region).

**Table S2. Abbreviated taxon nomenclature used in Figure 13 and corresponding full taxon and abundance information in soil and on PBAT film.**

| Abbreviated Taxon | Taxon | Abundance in Soil | Abundance on PBAT Film Surface |
|---|---|---|---|
| Acidobacteria 1 | Acidobacteria [Chloracidobacteria] RB41 | 0.0321 | 1.4931e-3 |
| Acidobacteria 2 | Acidobacteria Acidobacteria-6 CCU21 | 0.0138 | 1.28E-03 |
| Acidobacteria 3 | Acidobacteria Acidobacteria-6 iii1-15 | 0.064 | 5.87E-03 |
| Acidobacteria 4 | Acidobacteria Acidobacteria-6 iii1-15 mb2424 | 0.0103 | 1.32E-03 |
| Actinobacteria 1 | Actinobacteria Acidimicrobiia Acidimicrobiales | 0.029 | 5.24E-05 |
| Actinobacteria 2 | Actinobacteria Actinobacteria Actinomycetales Nocardioidaceae | 0.017 | 1.05E-04 |
| Actinobacteria 3 | Actinobacteria MB-A2-108 0319-7L14 | 0.0124 | 1.18E-04 |
| Actinobacteria 4 | Actinobacteria Thermoleophilia Gaiellales Gaiellaceae | 0.031 | 7.40E-03 |
| Actinobacteria 5 | Actinobacteria Thermoleophilia Solirubrobacterales | 0.0184 | 7.07E-04 |
| Actinobacteria 6 | Actinobacteria Thermoleophilia Other Other Other | 0.0118 | 3.93E-05 |
| Chloroflexi 1 | Chloroflexi Ellin6529 | 0.023 | 1.34E-03 |
| Firmicutes 1 | Firmicutes Bacilli Bacillales Bacillaceae Bacillus | 0.0143 | 3.67E-04 |
| Nitrospirae 1 | Nitrospirae Nitrospira Nitrospirales 0319-6A21 | 0.017 | 1.39E-03 |
| Proteobacteria 1 | Proteobacteria Alphaproteobacteria Rhizobiales | 0.0101 | 4.48E-03 |
| Proteobacteria 2 | Proteobacteria Alphaproteobacteria Rhizobiales Hyphomicrobiaceae | 0.0305 | 5.57E-03 |
| Proteobacteria 3 | Proteobacteria Alphaproteobacteria Rhizobiales Hyphomicrobiaceae Pedomicrobium | 0.0552 | 3.71E-03 |
| Proteobacteria 4 | Proteobacteria Alphaproteobacteria Rhizobiales Hyphomicrobiaceae Rhodoplanes | 0.0319 | 4.98E-03 |
| Proteobacteria 5 | Proteobacteria Alphaproteobacteria Rhodospirillales Rhodospirillaceae | 0.0321 | 5.17E-03 |
| Proteobacteria 6 | Proteobacteria Alphaproteobacteria Other Other Other | 0.03 | 1.61E-03 |
| Proteobacteria 7 | Proteobacteria Betaproteobacteria | 0.0188 | 1.48E-03 |
| Proteobacteria 8 | Proteobacteria Betaproteobacteria MND1 | 0.0295 | 2.49E-03 |
| Proteobacteria 9 | Proteobacteria Deltaproteobacteria Myxococcales | 0.0115 | 7.40E-03 |
| Proteobacteria 10 | Proteobacteria Deltaproteobacteria Syntrophobacterales Syntrophobacteraceae | 0.0147 | 1.93E-03 |
| Proteobacteria 11 | Proteobacteria Gammaproteobacteria Thiotrichales Piscirickettsiaceae | 0.0405 | 2.21E-03 |
| Proteobacteria 12 | Proteobacteria Gammaproteobacteria Xanthomonadales Sinobacteraceae | 0.0118 | 2.54E-03 |
| Other | Other | 0.0515 | 0.0219 |

**Table S3: Abbreviated taxon nomenclature used in Figure 14 and corresponding full taxon and abundance information in soil and on PBAT film.**

| Taxon | Abbreviated Taxon | Abundance in Soil | Abundance on PBAT Film Surface |
|---|---|---|---|
| Ascomycota Dothideomycetes Myriangiales unidentified unidentified Myriangiales sp | Ascomycota 1 | 0.1071 | 0.01 |
| Ascomycota Dothideomycetes Pleosporales Sporormiaceae Westerdykella Westerdykella sp | Ascomycota 2 | 0.0146 | 0.0605 |
| Ascomycota Eurotiomycetes Eurotiales Trichocomaceae Aspergillus Aspergillus fumigatus | Ascomycota 3 | 0.0132 | 1.66E-03 |
| Ascomycota Sordariomycetes Hypocreales Hypocreales fam Incertae sedis Acremonium Acremonium dichromosporum | Ascomycota 4 | 0.0647 | 0.0118 |
| Ascomycota Sordariomycetes Hypocreales Hypocreales fam Incertae sedis Acremonium Acremonium persicinum | Ascomycota 5 | 0.0103 | 6.98E-04 |
| Ascomycota Sordariomycetes Hypocreales Nectriaceae unidentified Nectriaceae sp | Ascomycota 6 | 0.0115 | 1.46E-03 |
| Ascomycota Sordariomycetes Hypocreales unidentified unidentified Hypocreales sp | Ascomycota 7 | 0.0178 | 0.0213 |
| Ascomycota Sordariomycetes Hypocreomycetidae ord Incertae sedis Plectosphaerellaceae Lectera Lectera longa | Ascomycota 8 | 0.0306 | 2.40E-03 |
| Ascomycota Sordariomycetes Microascales Microascaceae Microascus Microascus expansus | Ascomycota 9 | 0.0176 | 0 |
| Ascomycota Sordariomycetes Microascales Microascaceae Scedosporium Scedosporium prolificans | Ascomycota 10 | 0.0421 | 2.40E-04 |
| Ascomycota Sordariomycetes Microascales Microascaceae Scopulariopsis Scopulariopsis sp | Ascomycota 11 | 0.0864 | 1.96E-04 |
| Ascomycota Sordariomycetes Sordariales Chaetomiaceae unidentified Chaetomiaceae sp | Ascomycota 12 | 0.0162 | 2.14E-03 |
| Ascomycota Sordariomycetes Sordariales Lasiosphaeriaceae unidentified Lasiosphaeriaceae sp | Ascomycota 13 | 0.0329 | 3.21E-03 |
| Ascomycota Sordariomycetes unidentified unidentified unidentified Sordariomycetes sp | Ascomycota 14 | 0.021 | 0.0127 |
| Ascomycota unidentified unidentified unidentified unidentified Ascomycota sp | Ascomycota 15 | 0.1203 | 0.1504 |
| Basidiomycota Agaricomycetes Agaricales Psathyrellaceae Psathyrella Psathyrella sacchariolens | Basidiomycota 1 | 0.1869 | 2.18E-04 |
| Zygomycota Mortierellomycotina cls Incertae sedis Mortierellales Mortierellaceae Mortierella Mortierella amoeboidea | Zygomycota 1 | 0.0268 | 0.0127 |
| Unidentified Fungi sp | Unidentified | 0.055 | 0.0346 |